States of Selfstress in Diluted and Designed Square Tilings

Zandbergen, R.M.A.

States of Selfstress in Diluted and Designed Square Tilings.

R.M.A. Zandbergen November 29, 2019

Universiteit Leiden

Supervisors:
Dr. F.M. Spieksma
Prof.dr. M.L. van Hecke
A.S. Meeussen, MSc

Master thesis, Mathematical Institute, Leiden University

Contents

1 Introduction **5**

2 Main Theorem and algorithm **7**
2.1 Calculating states of selfstress 7
2.2 Finding states of selfstress using linear algebra 12

3 Theory **17**
3.1 Unit stresses 17
3.2 Smallest state of selfstress 19
3.3 Properties of larger states of selfstress 24
3.4 States of selfstress in tilings without holes: examples 30
3.5 States of selfstress in tilings with single holes: computation 31
3.6 States of selfstress in tilings with holes: examples 39

4 Creating holes: classifying the states of selfstress **47**
4.1 Single holes 47
4.1.1 Removal of a single tile in the tiling 47
4.1.2 Decrease and increase in the number of states of selfstress due to one hole of multiple tiles 49
4.2 Decomposing the tiling, holes at two or more tiles apart 51
4.3 Interference within tilings, holes at distances of one tile 53

5 Breaking corners **57**
5.1 Breaking apart connected corners in the tiling 57

6 Discussion **59**

Appendix A Definitions **61**

Acknowledgements **63**

Bibliography **65**

Chapter 1

Introduction

In this chapter we will introduce mechanical metamaterials. After this we will give a description of two properties of the materials considered in this thesis and explain the relation between metamaterials and the structures considered in this thesis.

As explained in [2], mechanical metamaterials are media that have properties depending on structure rather than the way these materials are composed. These materials are created by mankind, and can not be found in nature. The first structure that was created with metamaterial properties, was designed by R.S. Lakes in 1987, and has a negative Poisson's ratio [5]. This structure is depicted in Figure 1.1 and it contracts in all directions, when it is compressed in one direction, because of the way the unit cells of the material are constructed. This is in contrast with normal materials that extend in the other directions, when they are compressed in one direction, and thus have a positive Poisson's ratio. An example of this last case is a piece of rubber, because if we compress this piece of rubber on one side, the piece would be extending in the other two directions.

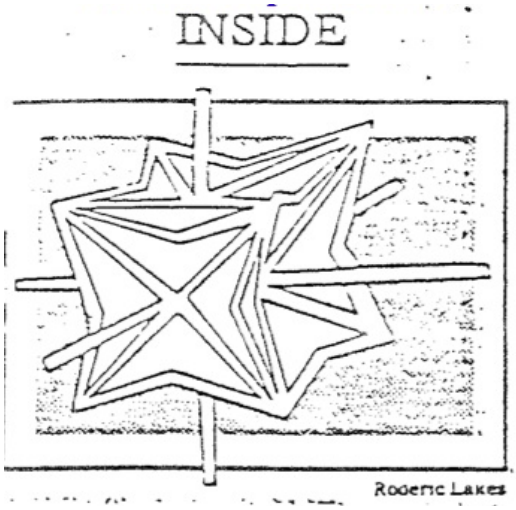

Figure 1.1: A unit cell of a material with a negative Poisson's ratio. This material will contract in all directions, when it is compressed in one direction. Edited from [4].

This thesis will consider a different kind of mechanical metamaterials, namely one consisting of squares connected at the corners. The square symmetry of the tiles (i.e. the independent squares) implies that the tiling is hingeable. We will give a description of the amount

of zero modes and states of selfstress of these tilings. These two notions give a description of how movable and rigid a tiling is, respectively. These two concepts are related to each other by the Maxwell-Calladine formula, which will be explained in Section 2.1. The amount of zero modes has been calculated for a large amount of tilings in the PhD thesis of Luuk Lubbers [6]. However, it turned out that for some tilings, it is difficult to determine the amount of zero modes. Using the Maxwell-Calladine formula, we can also start from the other direction and use the amount of states of selfstress to determine the amount of zero modes.

The PhD thesis of Luuk Lubbers is the only found source that presents some constraints on the number of states of selfstress on the square tiling. Apart from this thesis, there exist some notes, in which the first few examples of states of selfstress for this tiling are derived in both representations given in Section 3.2 and the example in Section 3.5 [8], the alternative Maxwell-Calladine formula for tilings without holes as written in 3.2 is given [10] and the general linear algebra explained in Section 2.2 is discussed [7]. Furthermore, it is known that it is possible to derive a rigidity matrix, from which the states of selfstress can be found by deriving the nullspace [8].

The goal of this thesis is to develop a method to determine the states of selfstress of these tilings, either using an algorithm that can be executed by hand or with an easy numerical calculation. Interestingly enough, we can show that any state of selfstress can be written as a linear combination of states of selfstress restricted to 3×3 subtilings. This also applies to tilings with holes, which we will show subsequently. We will determine the amount of states of selfstress for tilings with holes, and use this information to be able to determine the states of selfstress around these holes. As will be explained, these tilings with holes can be divided in different groups, for which it is possible to determine the states of selfstress. These different groups will be treated in Chapter 4. After this, we will also take a look at states of selfstress in tilings in which bonds are broken and discuss further research questions. In the appendix, a summary of all relevant definitions of this thesis is included.

Chapter 2

Main Theorem and algorithm

2.1 Calculating states of selfstress

In this section, we will introduce the definition of zero modes and states of selfstress. Furthermore, the Maxwell-Calladine counting formula will be discussed and this formula will be applied to the example tilings that we will study throughout this thesis. Finally, we will specify the problem that will be addressed in this thesis.

We will start with a couple of definitions.

Definition 2.1.1. *The degrees of freedom (or DOF) are the parameters in a system that can change independently of each other. The number of independent degrees of freedom will be denoted by* n_{DOF}.

Any point in a two dimensional plane has two degrees of freedom, namely the translations in the x- and y-direction in the xy-plane. Any rigid square in a two-dimensional plane has three degrees of freedom. These are the two translations in the x- and y-direction and the one rotation of the square, as depicted in Figure 2.1. These three degrees of freedom give all possible transformations of the square in the plane.

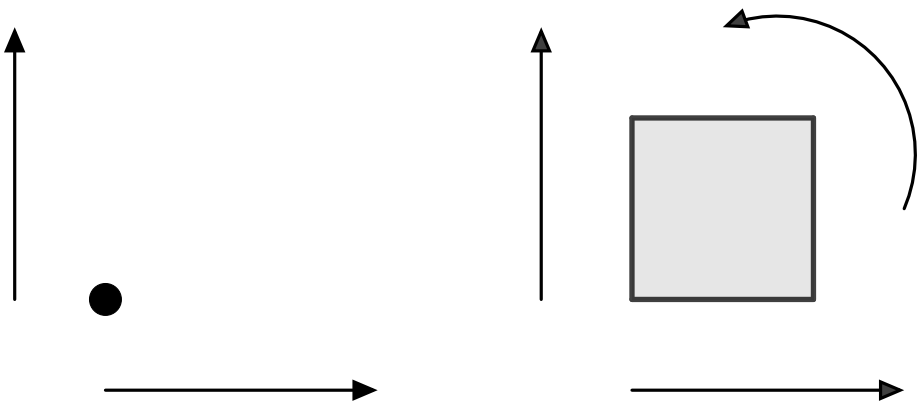

(a) (b)

Figure 2.1: All degrees of freedom for both a point and a square graphically represented. Applying these two or three transformations, respectively, give all possible transformations of the two elements.

Definition 2.1.2. *A restriction on the properties of different objects in a system is called a constraint.*

In our case, we will connect the different objects of the tiling, which will give constraints on the movements of the objects. We can for example connect two points in a two-dimensional plane by a stiff bar, see Figure 2.2. This gives one extra constraint on the degrees of freedom in the system: the distance between the two points is fixed. Thus there are 4 (2 DOF for each point) - 1 = 3 degrees of freedom, for the two points connected by one bar. These degrees of freedom are the two translations and the rotation of the bar. For the degrees of freedom of the assembled system, we have another notion: the zero modes of the system.

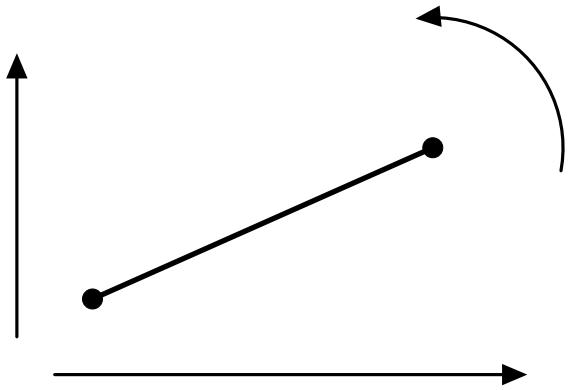

Figure 2.2: Two points connected by a stiff bar. The two points have four degrees of freedom, and there is one constraint (the distance between the two points is fixed). For the complete system, there thus are three global zero modes.

Definition 2.1.3. *The number of zero modes, free modes [10], relative mobility [3] or mobility, is defined as the number of independent parameters that can change without violating the constraints. The number of independent zero modes is denoted by* n_{ZM}*.*

Every object in two dimensions that consists of more than one point (i.e. there exists a direction in which its diameter is non-zero), always has at least three zero modes, the two translational zero modes, and one rotational zero mode. These will be called the *global zero modes*. If a system has additional zero modes, these are internal to the system, and thus will be called the *local zero modes*. In the case that there is one local zero mode in the system, the system will be called a *mechanism*.

As an example, consider the square in Figure 2.1b, which has no local zero modes: because there are no additional constraints on the square, we find that $n_{ZM} = n_{DOF}$. Thus the system only has the above described three global zero modes, and no additional local ones. Another example is shown in Figure 2.3a. In this system four bars are connected by frictionless joints to form a square. We see that the square is able to hinge over the joints, and thus there exist one local zero mode in this system, hence the system is a mechanism.

In the next part, we will give the definition of a state of selfstress of the tiling and use this to define a relation between all mentioned definitions.

Definition 2.1.4. *A state of selfstress in a system is a combination of forces over the elements in the system, that add up to a net force of zero.*

An example of a state of selfstress is shown in Figure 2.3b. If a force of size 1 is applied to

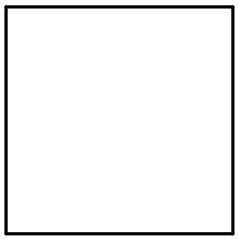

(a) A square, in which the nodes are frictionless joints. The system can hinge over these joints, and thus there is one local zero mode in the system. For this system holds: $n_{DOF} = 8$ and $n_{CON} = 4$.

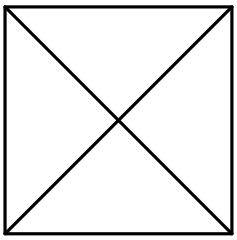

(b) Also in this square, the nodes are again frictionless joints. Because of the two cross bars, there is a state of selfstress in this system. Here, the following holds: $n_{DOF} = 8$ and $n_{CON} = 6$.

Figure 2.3: An example of (a) a local zero mode and (b) a state of selfstress.

the four 'boundary' bars, and a force of $-\sqrt{2}$ to the two cross bars, these forces cancel out and there is a force balance. Hence, this is a state of selfstress in the system.

In [9],[10], the Maxwell-Calladine counting formula between the four mentioned concepts is explained.

Theorem 2.1.5 (Maxwell-Calladine counting formula)**.**

$$n_{ZM} - n_{SSS} = n_{DOF} - n_{CON}, \tag{2.1}$$

where n_{ZM} is the number of zero modes or number of relative mobilities, n_{SSS} is the number of linearly independent states of selfstress, n_{DOF} is the number of degrees of freedom of the independent components of the system, when no constraints are added to the system, and n_{CON} is the number of constraints on these independent elements.

An explanation of the algebra behind this rule can be found in [1], and will be discussed in Section 2.2.

The number of degrees of freedom and the number of constraints of any system can always be determined by counting, but n_{ZM} and n_{SSS} can not be obtained in this way. To determine these, some concepts from linear algebra have to be used. We will explain these in Section 2.2. Luuk Lubbers [6], has calculated n_{ZM} numerically for several cases of the tilings we will be considering in this thesis and he has created a procedure, called iterative merging, to estimate n_{ZM} for large configurations.

The system considered in this thesis has square unit tiles. These unit tiles will be placed next to each other in such a way that two tiles connect at the corners. The connection between two tiles will also be called a *bond*. This is depicted in Figure 2.4 for a tiling of 4×6 elements. The numbering of the tiles is illustrated in Figure 2.5.

As explained above, each square has three degrees of freedom. Each connection between two nodes gives two constraints per tile: if the location of the first square is determined, for the second only a rotational degree of freedom remains, since the translational ones are fixed by the first square [10].

Example 2.1.6. For any complete $n \times m$ tiling, we find that there are $n \times m$ squares and thus $3(n \times m)$ degrees of freedom. It has $n \cdot (m-1) + (n-1) \cdot m$ connections, or because every

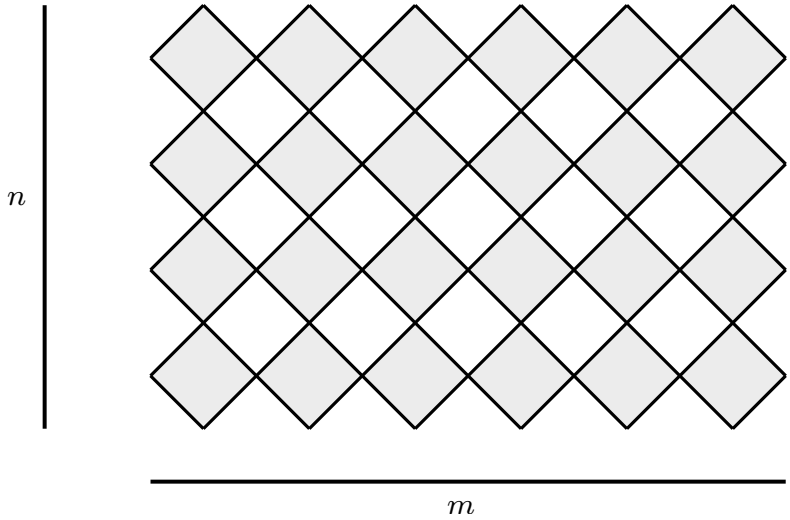

Figure 2.4: The system we are looking at. All tiles are connected to other tiles at the corners. For this Figure, we have $n = 4$ and $m = 6$. The amount of states of selfstress is determined explicitly for any n and m in Example 2.1.6.

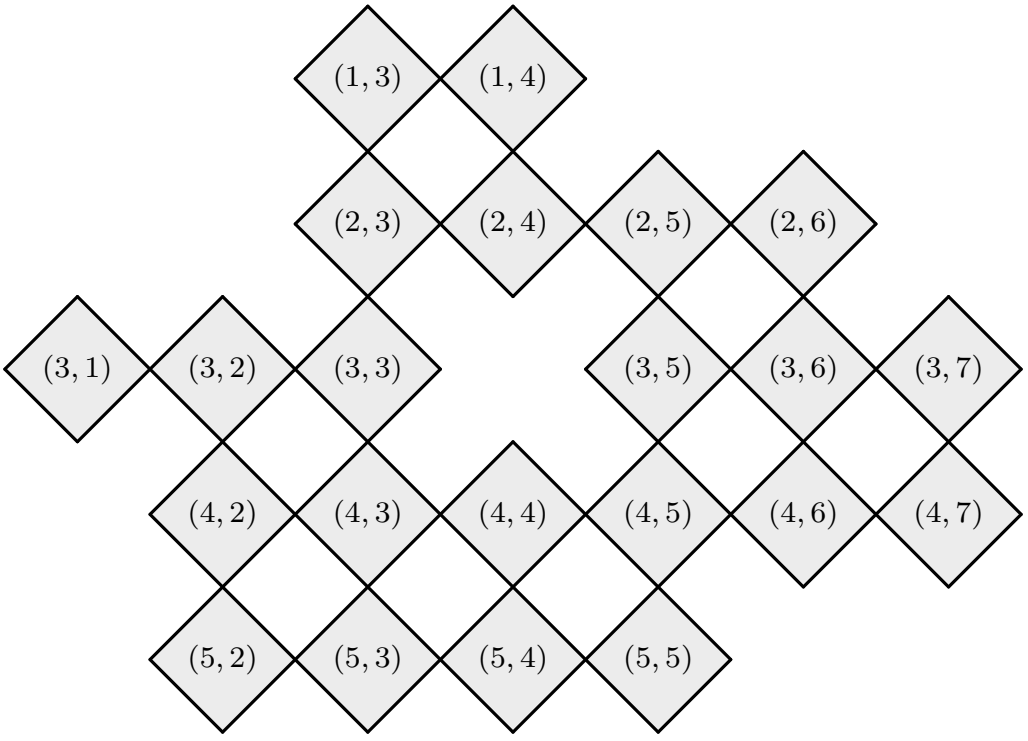

Figure 2.5: Enumeration of the different tiles. The counting of the rows starts at the uppermost row (this row can be incomplete) of tiles and continues downward. The counting of the columns is equivalent and goes from the left side of the tiling to the right side.

connection has two squares to which it is connected, $2 \cdot (n \cdot (m-1) + (n-1) \cdot m)$ constraints. As a consequence,

$$n_{ZM} - n_{SSS} = 3n \times m - 2 \cdot (n \cdot (m-1) + (n-1) \cdot m) = -(n-2)(m-2) + 4.$$

There always are three global degrees of freedom, and if both n and m are bigger than 1, there is one hinging mode, and thus $n_{ZM} = 4$. This results in $n_{SSS} = (n-2)(m-2)$.

The hinging mode comes from the fact that for every general, complete $n \times m$ tiling, with $n, m \geq 2$, there is only one possibility for the system to hinge freely (see Figure 2.6), which happens when we for example change the angle θ_1. In the case that there are not at least two squares next to each other in every direction, more complicated situations can arise, with more hinging modes. An example of this is depicted in Figure 2.7, which has four independent hinging modes.

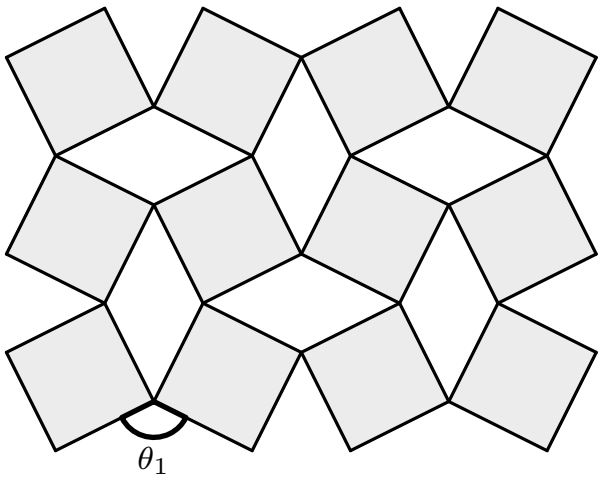

Figure 2.6: A 4×3 tiling that can be hinged freely, because the tiles are perfectly square. We can hinge the tiles by changing the angles between two squares, e.g. by changing the angle θ_1. Since this tiling is complete and $n, m \geq 2$, there is only one hinging mode. With Example 2.1.6, we then find that there exist two states of selfstress in this system.

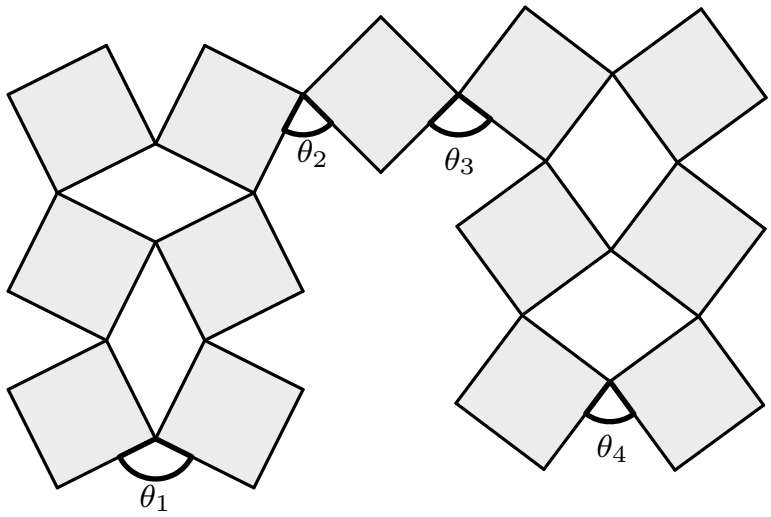

Figure 2.7: In this tiling all angles θ_i, for $i = 1, 2, 3, 4$ can hinge independent of each other. Thus, for this situation there exist more than one hinging mode. In total, there are seven zero modes in this tiling.

For any other tiling, we can equivalently determine the number of squares and the number of constraints by counting the number of squares and the number of bonds. With this, we can always determine the difference between n_{ZM} and n_{SSS}. But as Figures 2.6 and 2.7 show, the number of hinging modes is not always equal to one, and thus there does not always exist an easy-to-find solution when determining the states of selfstress or zero modes. In this thesis, we will derive an easier way to determine these states of selfstress. Using the Maxwell-Calladine counting formula, this also gives the number of zero modes of the tiling.

2.2 Finding states of selfstress using linear algebra

In this section, we will derive the so-called rigidity matrix. The transpose of this rigidity matrix describes a relation between the forces in the nodes and the forces internal to the bars. With this transpose matrix, we can determine all combinations of forces, such that the net forces in all nodes are zero, and thus find all states of selfstress in the tiling. To do so, we will look at displacements of the bonds between vertices and consider the axial and shearing components of the relative displacement, up to first order. As we will explain, the axial component is defined as the relative displacement of the vertices directed along the bond, and the shearing component is defined to be directed perpendicular to the bond.

Consider two nodes i and j, at locations $\vec{r}_i$ and $\vec{r}_j$ connected by a spring with length l^0, with length l_x in the x-direction and length l_y in the y-direction, as depicted in Figure 2.8.

Both nodes have a displacement $u_{x,k}$ in the x-direction and $u_{y,k}$ in the y-direction, for $k = i, j$, as depicted in Figure 2.8. For the spring we have the parameter bond extensions e_{ij} between the two nodes i and j. This extension does have one axial component, along the bond, and one shearing component, perpendicular to the bond.

We change the frame of view of this system in such a way that the spring is oriented in the

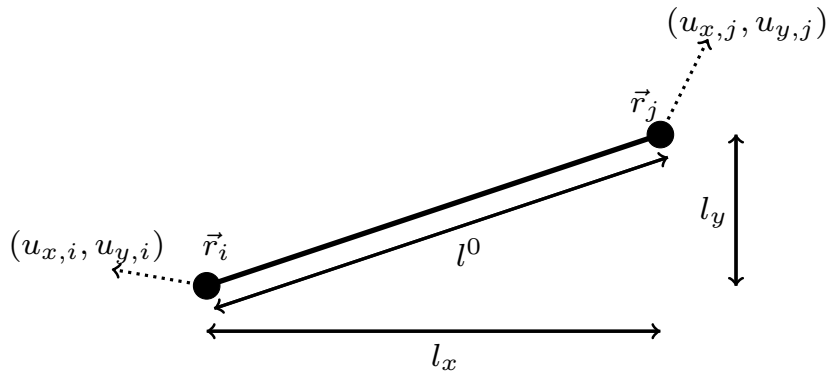

Figure 2.8: Two nodes i and j at r_i and r_j connected by a spring. The vector $d_k = (u_{x,k}, u_{y,k})$ denotes the displacement of the k-th node.

y-direction, to simplify the calculations [8]. There are two possible transformations for both nodes, namely translation and rotation.

An axial translation to the nodes (so a displacement along the bond) of equal size and the same direction for both nodes, is characterised by $u_{y,i} = u_{y,j}$ or $u_{y,i} - u_{y,j} = 0$. Violation of this constraint gives an axial strain $e_{ij,a} = u_{y,i} - u_{y,j}$ or, when rotated back to the general frame (up to first order approximation) [7]:

$$e_{ij,a} = \begin{pmatrix} \frac{l_x}{l^0} & \frac{l_y}{l^0} & -\frac{l_x}{l^0} & -\frac{l_y}{l^0} \end{pmatrix} \begin{pmatrix} u_{x,i} \\ u_{y,i} \\ u_{x,j} \\ u_{y,j} \end{pmatrix}. \tag{2.2}$$

To create a shearing strain in the system, we take two deformations of the system, that are both perpendicular to the bond. These two deformations are a transversal displacement, as in Figure 2.9a and a co-rotation in Figure 2.9b. For a small displacement, these two deformations add up to a shearing deformation, as depicted in Figure 2.10. Because of the small displacement, it is sufficient to look at the deformations up to linear order.

Here, we again make a coordinate transformation, so that the spring is again oriented in the y-direction. In the case that there is zero strain, so the transformations are in the same direction, up to first order it holds that: $u_{x,j} - u_{x,i} + \frac{l^0}{2}\theta_i + \frac{l^0}{2}\theta_j = 0$. Here, the rotation only affects half of the bond, and thus it is divided by 2. Violation of this constraint gives a shear strain in first order, equal to:

$$e_{ij,s} = u_{x,j} - u_{x,i} + \frac{l^0}{2}(\theta_i + \theta_j).$$

Rotating back gives, up to linear order:

$$e_{ij,s} = \frac{l_y}{l^0}(u_{x,j} - u_{x,i}) + \frac{l_x}{l^0}(u_{y,i} - u_{y,j}) + \frac{l^0}{2}(\theta_i + \theta_j).$$

Now we can combine the above strains, and obtain the strain matrix [7]:

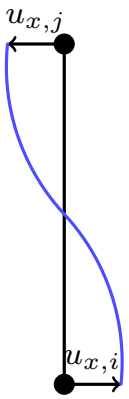

(a) The transversal displacement. Here $u_{x,i} = -u_{x,j}$.

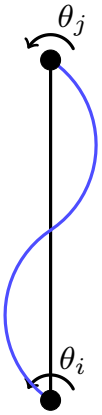

(b) The co-rotational displacement. Here $\theta_i = \theta_j$.

Figure 2.9: The two shearing displacements of the system. The blue edge represents the spring after the transformation.

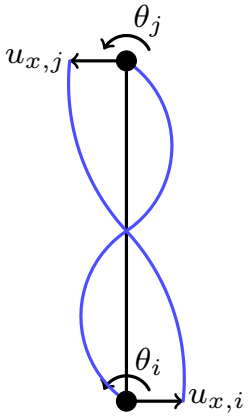

(a)

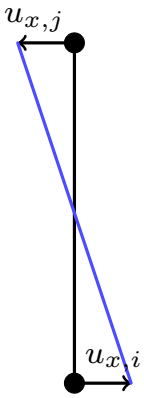

(b)

Figure 2.10: Up to linear order, a small co-rotation and small transverse displacement(a) will give a small rotation of the nodes(b).

$$\begin{pmatrix} e_{ij,a} \\ e_{ij,s} \end{pmatrix} = \begin{pmatrix} \frac{l_x}{l^0} & \frac{l_y}{l^0} & 0 & -\frac{l_x}{l^0} & -\frac{l_y}{l^0} & 0 \\ -\frac{l_y}{l^0} & \frac{l_x}{l^0} & \frac{l^0}{2} & \frac{l_y}{l^0} & -\frac{l_x}{l^0} & \frac{l^0}{2} \end{pmatrix} \begin{pmatrix} u_{x,i} \\ u_{y,i} \\ \theta_i \\ u_{x,j} \\ u_{y,j} \\ \theta_j \end{pmatrix}. \tag{2.3}$$

This relation can be extended to systems with more nodes and edges:

$$\begin{pmatrix} \vdots \\ e_{ij,a} \\ e_{ij,s} \\ \vdots \end{pmatrix} = \begin{pmatrix} & & & \vdots & \vdots & \vdots & & & & \vdots & \vdots & \vdots & & & \\ 0 & \dots & 0 & \frac{l_x}{l^0} & \frac{l_y}{l^0} & 0 & 0 & \dots & 0 & -\frac{l_x}{l^0} & -\frac{l_y}{l^0} & 0 & 0 & \dots & 0 \\ 0 & \dots & 0 & -\frac{l_y}{l^0} & \frac{l_x}{l^0} & \frac{l^0}{2} & 0 & \dots & 0 & \frac{l_y}{l^0} & -\frac{l_x}{l^0} & \frac{l^0}{2} & 0 & \dots & 0 \\ & & & \vdots & \vdots & \vdots & & & & \vdots & \vdots & \vdots & & & \end{pmatrix} \begin{pmatrix} \vdots \\ u_{x,i} \\ u_{y,i} \\ \theta_i \\ \vdots \\ u_{x,j} \\ u_{y,j} \\ \theta_j \\ \vdots \end{pmatrix} \tag{2.4}$$

or equivalently: $\vec{e} = R\vec{d}$, where R is the rigidity matrix [7], and $\vec{d}$ is the displacement vector of the nodes.

The nullspace of this matrix (vectors $\vec{d}$ such that $\vec{0} = R\vec{d}$) consists of the zero modes of the system. We can explain this by the fact that $\vec{0} = R\vec{d}$ consists of all displacement vectors such that the strain in the system remains zero. We know that the strain being zero, for a non-zero combination of displacement vectors, is a zero mode. Thus, the nullspace consists exactly of the zero modes of the system.

The transpose of this matrix describes a relation between the forces in the nodes $f_{x,i}$, $f_{y,i}$ and the forces internal to the bars σ_{ij}: $\vec{f} = R^T\vec{\sigma}$. The nullspace of this matrix gives the states of selfstress in the system, since $\vec{0} = R^T\vec{\sigma}$ consists of all vectors, such that the net force in the system will be zero.

Thus, to find the zero modes and states of selfstress of the system, we only have to construct the matrix R and then find the kernel and co-kernel of R, respectively.

We consider a variant of the transpose of the rigidity matrix, in which the bonds are depending on states of selfstress on 3×3 subtilings, as will be explained in Section 3.5. We then consider removed bonds in the tiling, on which the net force should be zero. The linear combinations of the states of selfstress on the 3×3 subtilings that result in a zero force, give the nullspace of the matrix. Thus, it is important to note that any state of selfstress in the system can be written as a linear combination of independent 3×3 states of selfstress.

Chapter 3

Theory

In this chapter, we will consider the states of selfstress in several tilings. As defined in Section 2.1, these states of selfstress are combinations of forces, such that all forces in the tiling add up to zero in both the horizontal and vertical directions. There are two possible ways to define the states of selfstress. In Section 3.1, we will discuss both of these ways. In Section 3.2, we will define the smallest tiling on which a state of selfstress exists and relate the two different ways to define the states of selfstress. In Section 3.3, we will consider the derivation of states of selfstress in more general systems.

3.1 Unit stresses

The states of selfstress on the tiling can be defined in two different ways. For the first one, that we will call representation [a], a stress balance on the centres of the squares is required, while for the second one, that will be called representation [b], there should be a stress balance on the corners of the squares. First of all, we will give the two representations. In Section 3.2 we will explain the relation between the two representations.

- In representation [a], we want a stress balance on the centres of the squares. Each square in this representation has three degrees of freedom, namely the two translations and one rotation. Two corners of different squares can be connected, and then we can apply forces between the centres of these two squares, running over the corners of the squares. These forces can be:
  - axial, or stretching, i.e. directed along the bond connecting the centres of two squares, or
  - shearing, which means that on one side of the bond, the stress is pushing in another direction than the stress on the other end of the bond.

  These different forces are depicted in Figure 3.1. An example of the shearing force and its effect on the tiles is depicted in Figure 3.2.

  The stretching and shearing forces, respectively, will be chosen in such a way, that they are opposite to each other, and have equal magnitude. As a result, these stretching and shearing forces add up to a net force of 0. This means that when two opposite axial forces (so two stretching forces, one with value -1 and one with value $+1$), or two opposite shearing forces are placed between the same two centres, they are

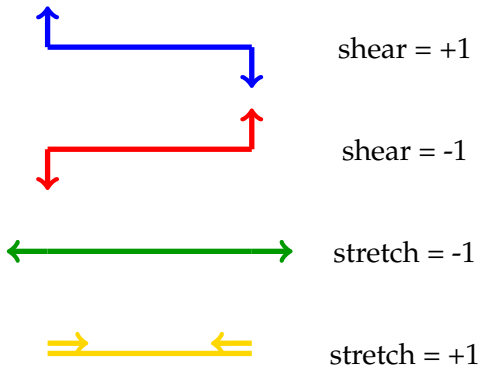

Figure 3.1: The different possible forces on the bonds in representation (a).

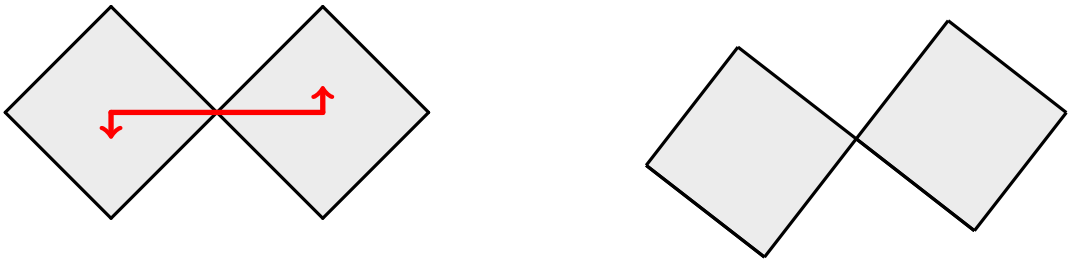

(a) (b)

Figure 3.2: Example of the situation with two shearing forces, and its influence on the squares. In (a) the force on the centres is represented. These forces are such, that both squares rotate the same (small) amount around the corner point where they are connected. The result of this rotation is depicted in (b).

in balance, and cancel each other. Also, if a shearing force and stretching force are placed together in a tiling as in Figure 3.3, these forces have to be balanced, and thus they have to point in the same direction, and have the same magnitude.

- In representation [b], we want a stress balance on the vertices of the squares. In this case, each separate vertex of the square has two degrees of freedom: the two translational directions. Every bond connects two vertices and gives one constraint on the system. The squares are connected at the vertices and the representation is defined in such a way, that in every direction the forces have to add up to zero. Using the projections on the x- and the y-directions, it is sufficient to check that the forces add up to zero in these directions.

  The forces in these squares only have attachment points on the corners of the squares, hence there are no points inside the squares that demand a force balance. Because of this force balance inside the squares, there have to be forces between the corners of the squares. There are two possibilities:

  - the forces between two corners next to each other within a square, and
  - the forces that are between two opposite corners within a square.

  We have depicted these two forces in Figure 3.4. Note that these two forces do not necessarily have to be extending, but can also be contracting.

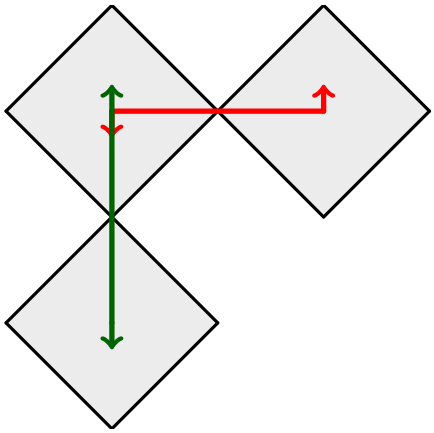

Figure 3.3: In the square in the upper left corner, the (green) tensional and the (red) shearing force are of equal size and exactly opposite to each other, and thus they cancel each other in the vertical direction, so that there is no stress in the square in the upper left corner.

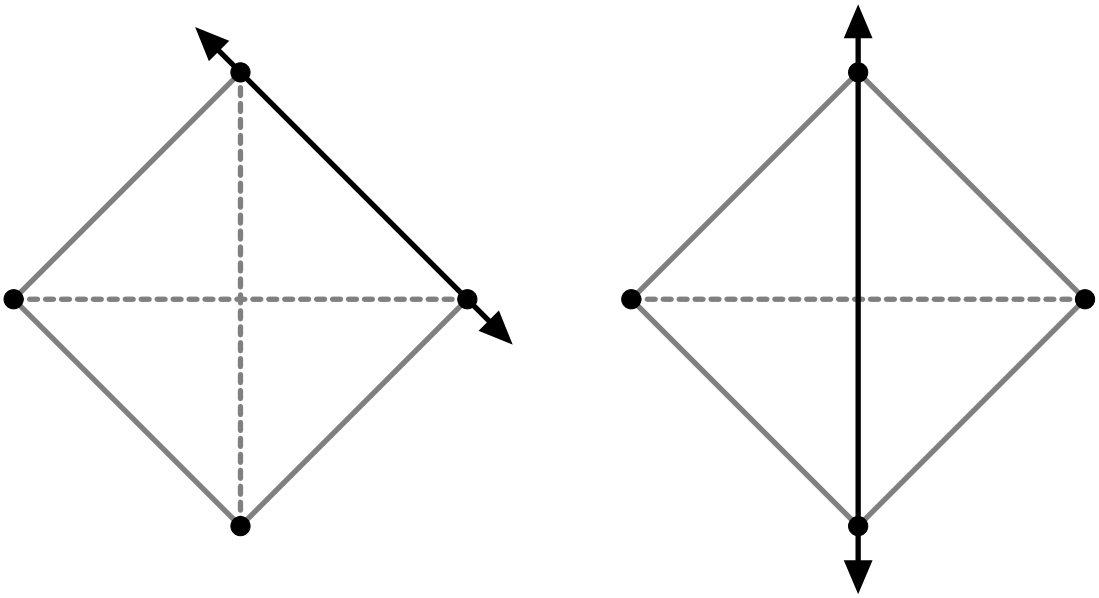

(a) A force between corners of the square that are next to each other.

(b) A force between two corners of the square, that are opposite to each other.

Figure 3.4: The two possible forces in representation [b], connecting corners of the squares along the edges.

3.2 Smallest state of selfstress

This section considers the smallest state of selfstress, i.e. the state of selfstress on the smallest tiling. For this, we first construct this smallest 3×3 state of selfstress. Then we will discuss how this state of selfstress is built up from smaller forces on the edges.

We start by defining the smallest state of selfstress possible in the tilings. For this, we first consider a tiling with 4 squares (see for an example Figure 3.5). In this case, counting gives

4 squares and 4 connections. Furthermore, there are three global zero modes. Of course, we also see, that we can change the angle θ_1 between the squares, because the squares are perfect rectangles. From this it follows, that there is one local zero mode.

By counting we thus get:

$$n_{ZM} - n_{SSS} = n_{DOF} - n_{CON} = 3 \cdot 4 - 2 \cdot 4 = 4.$$

We have already seen that $n_{ZM} = 4$, and thus, we see that there are no states of selfstress in the 2×2-tiling. Using an analogous proof, it can be shown, that there neither are states of selfstress in any $1 \times n$-, $n \times 1$-, $2 \times n$- or $n \times 2$-tiling.

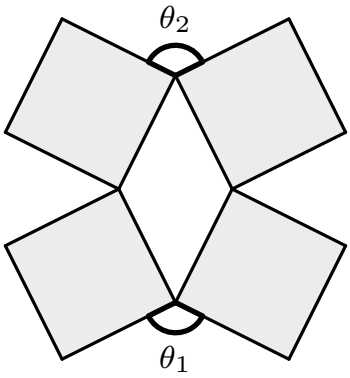

Figure 3.5: These four squares have four zero modes. Three of them are global and one is a local zero mode, the hinging mode of the total system. The two angles θ_1 and θ_2 remain equal to each other, while hinging.

For the situation of Figure 3.6, counting gives

$$n_{ZM} - n_{SSS} = n_{DOF} - n_{CON} = 3 \cdot 8 - 2 \cdot 10 = 4.$$

From this, we again obtain the same zero modes as defined above: three global zero modes and one hinging zero mode of the system.

Since the tiles are perfect squares, this implies that the distance between the two points a_1 and a_2 remains the same. This implies that adding another square tile, of which two of the neighbouring corners are at a_1 and a_2, does not change the number of zero modes. But then we have that:

$$4 - n_{SSS} = n_{DOF} - n_{CON} = 3 \cdot 9 - 2 \cdot 12 = 3,$$

from which follows that a 3×3 tiling contains one state of selfstress.

This suggests that the smallest amount of square tiles in which a state of selfstress can be found, is a 3×3 tiling, to which we will also refer as the 3×3 state of selfstress. For this 3×3 tile, the state of selfstress in the two different representations is depicted in Figure 3.7.

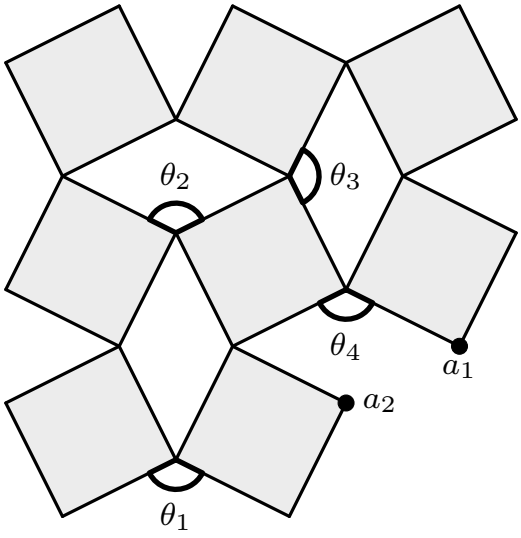

Figure 3.6: These eight squares again have four degrees of freedom. Two of them are translational, one is rotational and one is the hinging mode. The angles $\theta_1, \theta_2, \theta_3$ and θ_4 remain equal to each other, while hinging. Since the tiles are perfect squares, the distance between a_1 and a_2 remains equal when the system is hinging.

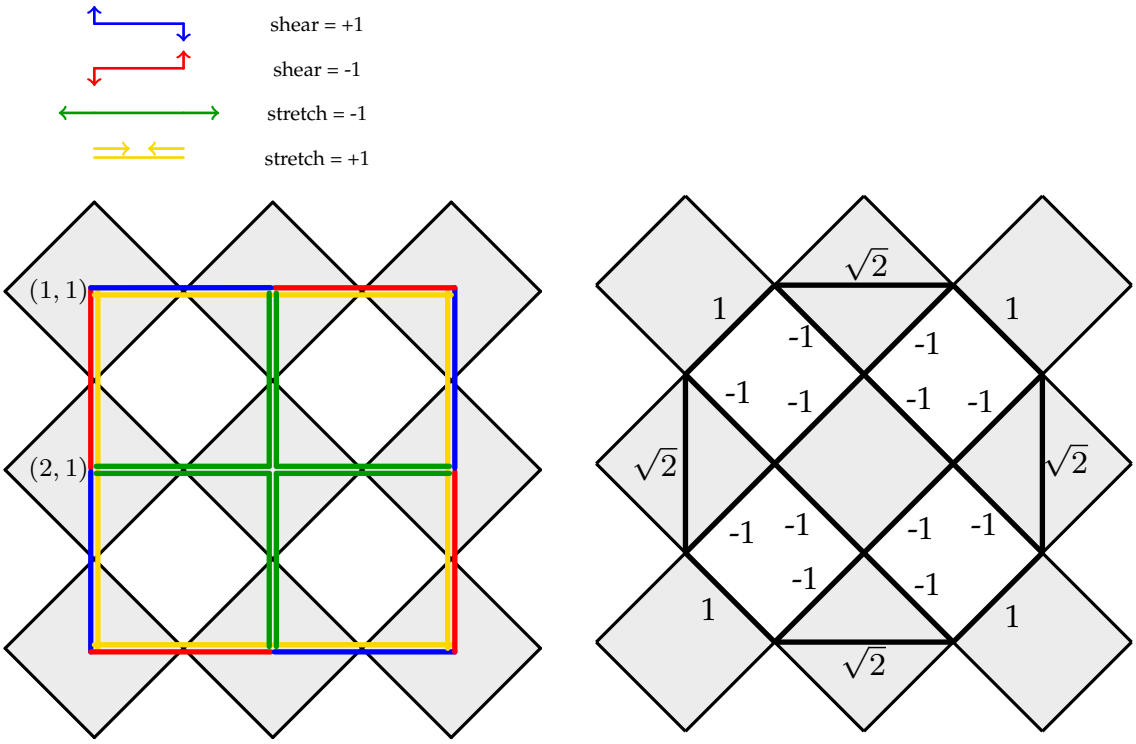

(a) 3x3 tiling in representation [a].

(b) 3x3 tiling in configuration [b].

Figure 3.7: 3x3 tiling in the two defined configurations.

Theorem 3.2.1. The 3×3 state of selfstress in representation [b] is unique up to a constant, with forces of magnitude ± 1 for edges connecting two adjacent corners and forces of magnitude $\pm\sqrt{2}$ for edges connecting two opposite corners.

Proof. We already know that there is a unique state of selfstress in the 3×3-tiling, and that this one is represented in Figure 3.7. From representation [b] it follows, that up to a constant multiplication factor of the whole tiling, there can only be forces equal to ± 1 for edges connecting two adjacent corners and $\pm\sqrt{2}$ for edges connecting two opposite corners. □

The above theorem implies that in every tiling there can be two different forces over the edges: the forces over edges between opposite corners; and over the edges connecting two adjacent corners. Using this, we will show that any tile with non-zero forces can be decomposed into two smaller basis tiles, that either consist of a force between opposite corners, or a force between two corners next to each other. This second case can for example be found in the $(1, 1)$-tile (the tile in the upper-left corner) for both representations in Figure 3.7. These basis tiles, with a force between opposite corners or a force between two corners next to each other, are shown for both representations in Figure 3.8. The forces on the bonds in representation [a] are shown in Figure 3.9a. It is also possible to consider these forces with respect to the centres of the tiling, in which case the forces on the corners are given as in Figure 3.9b. The combination of these forces at the corners gives the remaining net force, shown in Figure 3.9c. This remaining net force is depicted in Figure 3.8b.

(a) The first basis tile in representation [a].

(b) The first basis tile in representation [b].

Figure 3.8: The first basis tile, taken from tile $(1, 1)$, the upper left corner, of Figure 3.7.

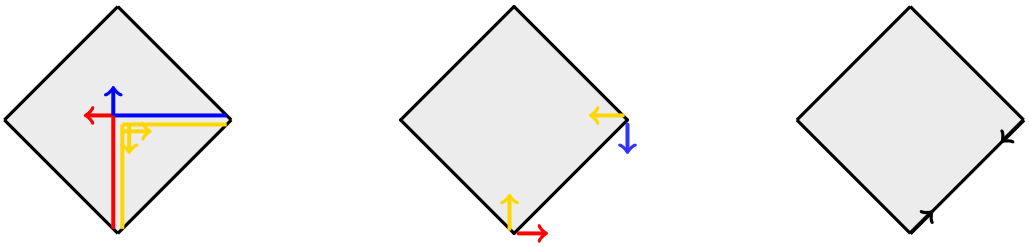

(a) Forces of the first basis tile in representation [a]. Here, the arrows are corresponding to these forces.

(b) The forces seen relative to the center of the squares.

(c) Net force remaining from the forces in Figure 3.9b. We will assume that the magnitude of the force on this vector is equal to 1.

Figure 3.9: Translation of the forces in representation [a] to the forces in representation [b]. First of all, we will consider the forces seen from the centres of the squares (b). These forces are subsequently used to calculate the net force on the corner points as shown in (c), which gives representation [b].

Secondly, we consider the square $(1, 2)$ of Figure 3.7. If we add the basis tile from Figure 3.8 and this same basis tile under a rotation over 90 degrees in a counterclockwise direction, we obtain the situation with forces between opposite corners, as shown in Figures 3.10a and 3.10b. It is again possible to define a relation similar to the one in Figure 3.9 between these two representations. In this case, we take the forces in the second representation of size equal to $\sqrt{2}$, in order to compensate the forces of Figure 3.8b.

(a) The second basis tile in representation [a]. (b) The second basis tile in representation [b].

Figure 3.10: The second basis tile.

Using these two tiles, we can construct any other tile, by linear combinations of these two squares in Figure 3.8 and in Figure 3.10. In doing so, we only have to use integer combinations of the two tiles to construct any of the other possible tiles. We will prove this.

Theorem 3.2.2. The force on every tile can be written as a linear combination of the two basis tiles represented in Figure 3.8 and in Figure 3.10, and their rotations.

Proof. Consider representation [b]. Since all forces in this representation are between corners of tiles, the possible forces can only be over edges connecting two adjacent corners and over edges connecting two opposite corners. It is trivial, but tedious to check that for all combinations of forces, the two tiles represented in Figures 3.8b and 3.10b, with all rotations that give a different configuration, give all these possible forces on the tile. Thus we can write the forces on any tile as a linear combination of the forces on these two tiles. By a good choice of the force of the first edge, all other forces on the edges of the tiles will be integer combinations of the two tiles represented in Figures 3.8b and 3.10b.

Equivalently, this can be done for representation [a], but now using that the forces must be connecting the centres of the squares. □

There does not exist a bijective image between these two representations and thus this is not sufficient to get unicity. To get unicity, we have to use the tile in Figure 3.11. This tile is important, because it is the unique tile for which in each of the four corners the forces compensate each other and thus it is the unique tiling for which the resulting force on the tiling is zero. This tile can be added to any tile of any tiling, without requiring to change the forces on tiles located next to this tile. From this, it follows that the resulting force on the square is zero. It is thus possible to add this unit tile to any tile in representation [b], without changing the state of selfstress. Thus, the forces on every tile are unique up to a constant multiple of the forces on this unit tile. As a result, we see that there exist multiple ways to represent a square in the tiling in representation [b].

The relation between the two basis tiles, represented in Figure 3.8 and in Figure 3.10 in combination with the unit tile, implies the following corollary to Theorem 3.2.2:

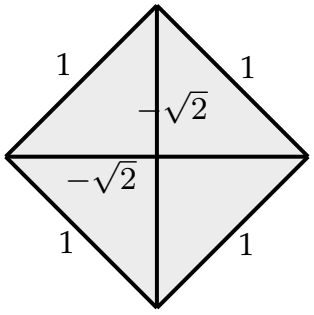

Figure 3.11: Force balance in all four corners of the square of the unit tile. Because all forces compensate each other inside the square, they can be removed.

Corollary 3.2.3. Up to addition of the unit tiling, there exists a bijection between the tilings in the two representations.

3.3 Properties of larger states of selfstress

In this section, we will show that we can write any state of selfstress in both tilings with and without holes, as a linear combination of the states of selfstress on 3×3 subtilings of the tiling as defined in Section 3.2, with all holes filled up. To do so, we will first consider tilings without holes, and show that the number of linearly independent states of selfstress, n_{SSS}, equals the amount of 3×3 subtilings in the tiling. After this, we will prove that in any tiling with holes, we can write any state of selfstress as a linear combination of 3×3 states of selfstress on the tiling with the holes filled up. If a state of selfstress can not be written as a linear combination of two states of selfstress on a smaller tiling, i.e. tilings containing less squares, we will call this state of selfstress a *basis state of selfstress.* In general, all local 3×3 subtilings in a tiling are basis states of selfstress.

We will first define the boundary of the tiling, which we will call the polygon boundary.

Definition 3.3.1. *The polygon boundary is the smallest binding polygon with horizontal and vertical edges, for which both endpoints of the edges are in the centres of (expected) holes.*

An example of this polygon boundary is shown in Figure 3.12. This polygon boundary can be used in two ways: to determine the amount of corners of the tiling at the polygon boundary, which can be used to obtain an alternative version of the Maxwell-Calladine counting formula. Secondly, the polygon boundary can be used to obtain the amount of 3×3 subtilings in the larger tiling and thus be used to show that in a large tiling, all linearly independent 3×3 states of selfstress are positioned on the 3×3 subtilings of the tiling.

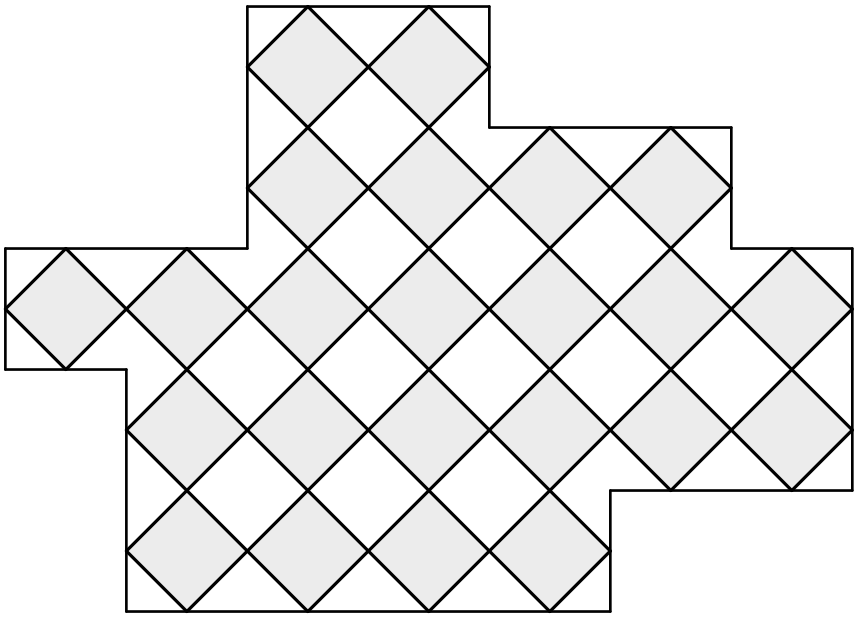

Figure 3.12: A tiling with the polygon boundary of this tiling.

First, we derive a variant of the relation between n_{SSS} and n_{ZM}, in terms of the number of tiles, and the number of corners at the polygon boundary of the tiling. Note that every corner of a tile is either connected to another corner, or it is at the outside, and thus connected to the polygon boundary.

Assume that a tiling has N tiles, and that the n-th tile has c_n corners connecting to other tiles. The number of corners of the n-th tile located at the polygon boundary, is defined by b_n and equal to $b_n = 4 - c_n$. Taking all of these together, we get: number of connections $= \sum_{n=1}^{N} c_n = \frac{4N-B}{2}$, where $B = \sum_{n=1}^{N} b_n$ is the total number of corners of all tiles at the polygon boundary of the tiling. We divide by 2, because every connection is counted twice. Since the number of constraints is twice the number of connections, we get that the number of constraints is equal to $4N - B$. Thus:

$$n_{SSS} = n_{CON} - n_{DOF} + n_{ZM} = 4N - B - 3N + n_{ZM} = N - B + n_{ZM}. \tag{3.1}$$

This equation can be used to determine the amount of states of selfstress, using the amount of tiles, the amount of corners of independent tiles at the boundary and the amount of zero modes. An example of this is the following.

Example 3.3.2. Consider the particular case in which there are no holes in the tiling, as well as no single bonds between subtilings, i.e. breaking one bond in the tiling should preserve the connectedness of the tiling.This last constraint implies that there are no additional zero modes in the tiling, so that the number of zero modes is equal to 4. These four zero modes are the three global zero modes for the movement of the system and the hinging mode of the system, as explained in Section 3.2. Thus we get that:

$$n_{SSS} = n_{CON} - n_{DOF} + n_{ZM} = 4N - B - 3N + 4 = N - B + 4. \tag{3.2}$$

More generally, Equation 3.1 also holds when there are holes in the tiling, i.e. some of the squares in the center of the tiling are removed. In this case, more complicated constraints

on the number of single connections are needed, implying that no additional zero modes appear in the tiling, when removing the tiles. These constraints will be discussed in Chapter 4. In Figure 3.13 an example of this case is shown. Here, the tiling does not contain any additional zero modes, there is one state of selfstress in this tiling, but there are no 3×3 states of selfstress in this tiling. It will be shown that states of selfstress like this one are located on the tiles surrounding the holes in the tiling.

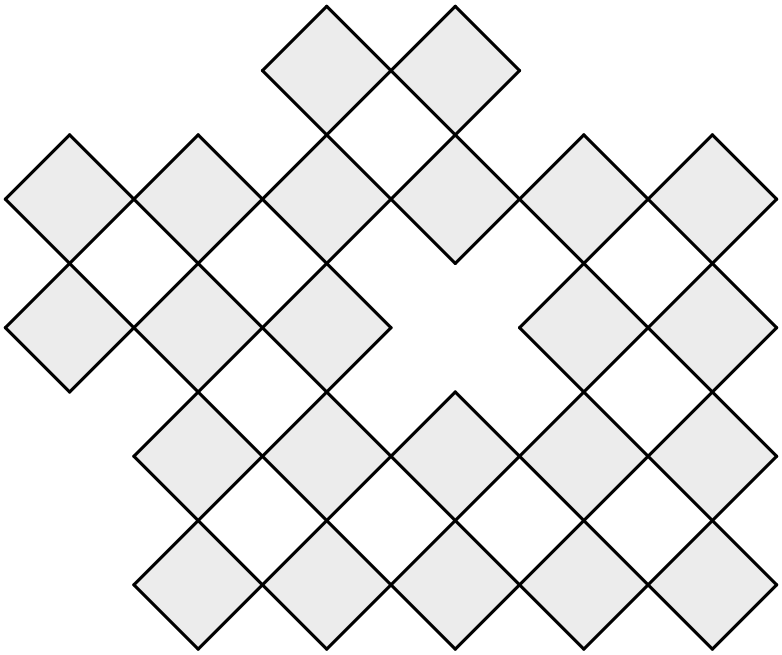

Figure 3.13: This tiling contains only 4 zero modes, because there is only one site in the tiling with only one connection between the outer boundary and the hole. In this tiling there are no 3×3 subtilings containing a state of selfstress, but counting ($N = 23$, $B = 26$) gives that there exists one state of selfstress. Since we know that states of selfstress are not available on tilings of the size $1 \times n$, or $2 \times n$, as seen in Section 3.2, the state of selfstress has to surround the hole in the tiling, as we shall see later.

The idea of finding the states of selfstress in tilings with holes is as follows: when we fill the holes in the tiling with squares, we can define 3×3 states of selfstress with forces going over the squares placed in the holes. Considering all different combinations of 3×3 states of selfstress with the total force over all edges of this added squares being zero, will give all states of selfstress in the tiling with holes. In this case, we will call the 3×3 states of selfstress containing a part of the holes, that are contributing to the larger state of selfstress with zero force on the bonds covering the holes, 3×3 *covering states of selfstress*.

We will now prove the validity of the above statements, i.e.

a. If there a no holes in the tiling, then n_{SSS} equals the number of 3×3 subtilings. As a result of this, we will call all states of selfstress that are located on 3×3 tilings, either 3×3 subtilings or local 3×3 states of selfstress.

b. In a tiling with holes, every state of selfstress can be written as a linearly independent combination of 3×3 states of selfstress. These independent states of selfstress may have a non-zero force on the bonds connecting the removed tiles, but a combination of these 3×3 covering states of selfstress should result in a net force of zero on the removed bonds.

In Section 3.4, we discuss examples of tilings without holes, in Section 3.5 the case with holes will be worked out for two examples: the 5×5 tiling, with a 1×1-sized hole in the centre and a comparable example to the situation in Figure 3.13.

To prove the first statement, we consider tilings without holes. Based on Equation 3.1, we want to prove that the amount of tiles that are located in the center of 3×3-subtilings is equal to the number of 3×3 states of selfstress, which equals $N - B + n_{ZM}$. For these tilings, we want to determine the number of 3×3 subtilings within the tiling, that can also be found by considering the number of squares surrounded by eight other squares. Since these tiles are the complement of the tiles that are not surrounded by eight other tiles, we can alternatively count these tiles. To this end, we will consider the polygon boundary and the corners of this polygon boundary, and divide these in two different groups:

- There are the sides of the polygon boundary for which at least two corners of one tile are on the polygon boundary. This tile is counted at least twice, when counting the number of squares at the polygon boundary. These corners will be labeled with a $+$.
- On the other hand, there are tiles that are neither connected to the boundary, nor surrounded by eight other tiles. These tiles occur at corners for which only two tiles contribute to the boundary. These corners are denoted by a $-$.

This division into the different corners is performed in Figure 3.14 for the tiling of Figure 3.12. Note that for a tiling without holes, there are our more $+$-corners compared to the amount of $-$-corners. This can equivalently be done for the case when there are holes in the tiling. In this case, we have to construct polygons, that can be placed inside the tiling and do not contain tiles of the tiling. The union of the enclosing polygons will then form the polygon boundary of the tiling. Note that every additional hole will add four more $-$-corners compared to the amount of $+$-corners to the boundary. Using the amount of squares at the boundary we can show that the amount of tiles at the boundary equals the number of 3×3 states of selfstress, minus the amount of zero modes in the tiling.

Theorem 3.3.3. If a tiling does not contain any holes, the amount of squares at the polygon boundary equals $B - n_{ZM}$.

Proof. The number of squares at the polygon boundary can be written as:

$$\begin{aligned} \#\text{ of squares at boundary} &= B + \#\text{ of } - \text{-corners} - \#\text{ of } + \text{-corners} \\ &\quad - \#\text{ of twice-counted tiles at the polygon boundary} \\ &= B - 4 - \#\text{ of twice-counted tiles at the polygon boundary.} \end{aligned}$$

These tiles at the polygon boundary are counted twice, because of the fact that they are connected to the polygon boundary at two sides of the tile, while the polygon boundary is not surrounding the tile. This occurs when the tiling has single bonds between two subsets of tiles, and this thus gives additional zero modes. This can for example be seen in the tiling in Figure 3.14. Here, the blue-dotted tile is surrounded by the polygon boundary on two sides and thus counted twice. Apart from the four global hinging modes, each double-counted square represents an extra hinging mode of the tiling. This can be concluded from the fact that each tile that is surrounded by the polygon boundary on different sides, corresponds to a single connection between components, that can move independently of other components.

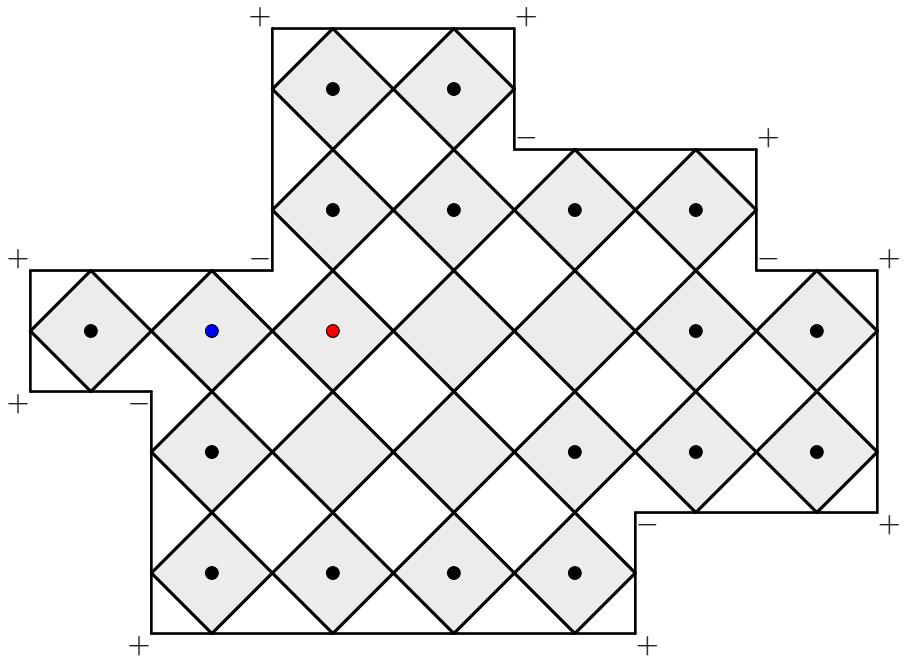

Figure 3.14: The tiling with boundary elements and orientation of the corners. All dotted tiles are located at the polygon boundary. For the $+$-corners, one tile is counted two times, while for the $-$-corners, one extra tile is at the boundary. In the case that there are no holes in the tiling, we see that there always are 4 more $+$-corners than there are $-$-corners. The square (3,3) denoted in red, is located at the polygon boundary, because it is not surrounded by 8 squares.

Thus we get, since we have to subtract the global hinging mode and the translational modes: # of twice-counted tiles at the polygon boundary $= n_{ZM} - 4$ and we find for the number of squares at the boundary:

$$\begin{aligned} \#\text{ of squares at boundary} &= B - 4 - \#\text{ of twice-counted tiles at the polygon boundary} \\ &= B - 4 - (n_{ZM} - 4) \\ &= B - n_{ZM}. \end{aligned}$$

□

Theorem 3.3.4. If a tiling does not contain holes, every state of selfstress in this tiling can be written as a linear combination of independent states of selfstress over 3×3 subtilings, resulting in $n_{SSS} =$ number of 3×3 subtilings.

Proof. The number of states of selfstress can be found with Equation 3.1, which gives $n_{SSS} = N - B + n_{ZM}$. Here, the amount of zero modes depends on the amount of single bonds between sublattices, which enable two sublattices to hinge independently from each other.

Since the number of squares at the boundary equals $B - n_{ZM}$, as derived in Theorem 3.3.3, the number of tiles not located at the boundary, and thus the number of 3×3 subtilings equals $N - B + n_{ZM}$. This is equal to the number of independent states of selfstress in the tiling. Since every 3×3 tiling corresponds to an independent state of selfstress, the states of selfstress and the 3×3 subtilings have to be the same. With this, it is possible to write every state of selfstress in the tiling as a linear combination of the linearly independent 3×3 states of selfstress. □

Next, we will consider a tiling with holes. As was explained before, we can write any state of selfstress as a linear combination of 3×3 states of selfstress with the holes in the tiling filled up with squares. This will be proven in the following theorem.

Theorem 3.3.5. Every basis state of selfstress on a general tiling is either a linear combination of 3×3 covering states of selfstress or a 3×3 state of selfstress, i.e. it is a linear combination of 3×3 states of selfstress.

Proof. Consider a tiling with holes in it, and if there is one contained in the tiling, a state of selfstress. Now, there are two situations: the state of selfstress is on a tiling that only consists of 3×3 subtilings, or it is not. The first case is trivial, because by Theorem 3.3.4, the statement follows. In the second case, the state of selfstress has to be surrounding a hole. Putting a tile with zero forces in the holes gives a complete, admissible tiling. Since we know that any state of selfstress on a complete tiling can be written as a linear combination of 3×3 states of selfstress by Theorem 3.3.4, this thus gives that the state of selfstress surrounding these filled up holes also have to be linear combinations of 3×3 states of selfstress. Thus we find that every state of selfstress can be written as a linear combination of 3×3 states of selfstress. □

The next corollary gives a result of the scaling factors of the states of selfstress and shows that any state of selfstress can be written with forces that are integer multiples of 1 and $\sqrt{2}$, for a right choice of scaling factors.

Corollary 3.3.6. Every basis state of selfstress on a general tiling can be written as an integer linear combination of the 3×3 states of selfstress. For the right choice of multiplication factor, every force in the state of selfstress, is an integer multiple of 1 if the force goes over an edge connecting two adjacent corners in a square and an integer multiple of $\sqrt{2}$, if the force goes over an edge connecting two opposite corners.

Proof. Let a basis state of selfstress be given. If the tiling only consists of 3×3 subtilings, it is tedious but easy to verify that by the right choice of the prefactor, we only have the 3×3 states of selfstress of Figure 3.7b. As proven in Theorem 3.2.1, the corollary holds in this case. In the situation that the tiling does not only consist of basis states of selfstress that are 3×3 states of selfstress, there must be a state of selfstress surrounding a hole. But since the combination of 3×3 states of selfstress needs a force of value zero in the holes, the basis state of selfstress surrounding the hole has to be an integer linear combination of the 3×3 covering states of selfstress. By the right choice of a multiplication factor, the forces over edges connecting two adjacent corners in a square are an integer multiple of 1 and forces over edges connecting two opposite corners are an integer multiple of $\sqrt{2}$. The deduction of this is again tedious, but easy. □

3.4 States of selfstress in tilings without holes: examples

The results of the previous section can be extended to larger systems. This section will give a couple of examples of this extension, and in the third example, we will show how the reasoning of Section 2.2 can be applied to find states of selfstress in the system.

Example 3.4.1. First consider an $n \times m$ tiling, with $n, m \geq 3$. We have derived that there are $(n-2)(m-2)$ linearly independent local states of selfstress. By virtue of Theorem 3.3.4, these $(n-2) \times (m-2)$ states of selfstress are located on the independent 3×3 subtilings in the $n \times m$ tile. All other states of selfstress can be found to be a linear combination of these local states of selfstress.

Example 3.4.2. Using Equation 3.1 for a tiling without holes in the tiling, gives $n_{SSS} = N - B + n_{ZM}$, where N the number of squares, B the number of boundary elements, and n_{ZM} the number of zero modes. We find for the example in Figure 3.15 that there is one single bond, between the leftmost square, numbered $(3, 1)$ and the squares more to the right. This gives an additional zero mode, so that there are 5 zero modes in the tiling and thus there are four states of selfstress. As derived in Theorem 3.3.4, these all have to be 3×3 states of selfstress located on 3×3 subtilings, since there are no holes in the tiling. These four states of selfstress are denoted with different colours in Figure 3.15.

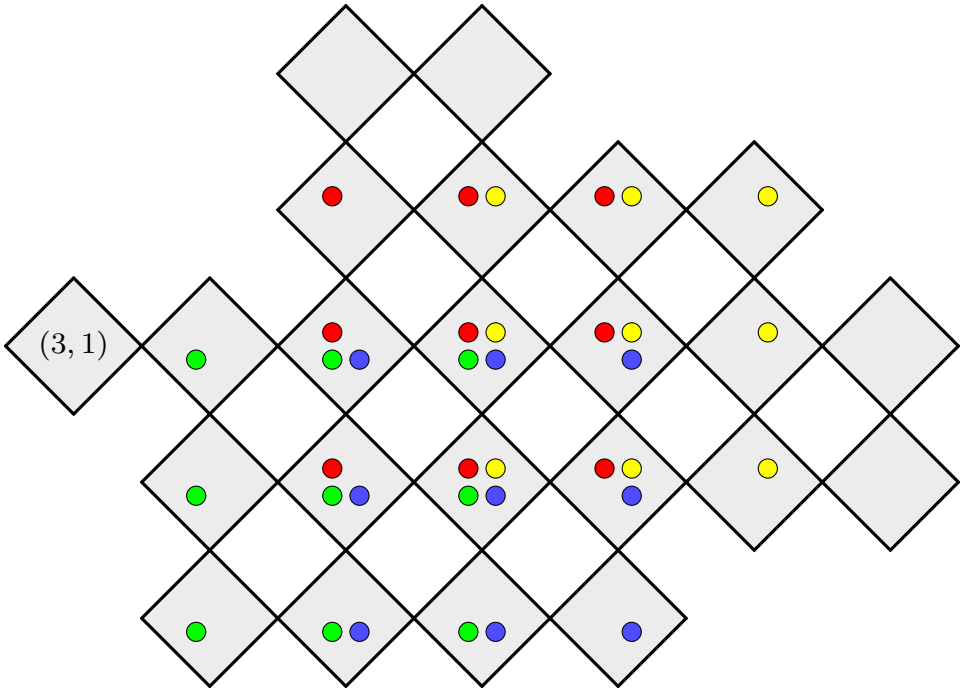

Figure 3.15: Example for counting the amount of states of selfstress, using the amount of boundary elements of the tiling. In this situation, there are 23 squares, 24 boundary elements and 5 zero modes. Thus, in total there are 4 independent 3×3 states of selfstress. These four are depicted with four different colours in the figure.

3.5 States of selfstress in tilings with single holes: computation

In this section, we will consider tilings with holes. In general, we will assume that the tiling is relatively small, compared to the hole in the tiling, so that there are no 3×3 basis states of selfstress. We start with a simple example of a tiling that has a hole in its centre and we will give the linearly independent states of selfstress of this tiling. After this, we will consider a mechanism to construct the states of selfstress using a small variant of the approach explained in Section 2.2. We will apply this approach to the example, show that this gives the states of selfstress defined before and give an algorithm to determine the states of selfstress of a more general tiling. After this, we will consider multiple examples to illustrate the different types of states of selfstress that can appear around one or multiple holes.

Example 3.5.1. The first example of a tiling with a hole is a 5×5 tiling, with the $(3, 3)$-square, i.e. the centre square removed. This tiling contains 24 squares and 24 boundary elements and thus $n_{ZM} - n_{SSS} = 0$. The amount of zero modes equals 4, because this system only contains global zero modes. Thus there are 4 independent states of selfstress, that are represented in Figures 3.16-3.19. The construction of the basis states of selfstress of this tiling will be discussed after the Figures.

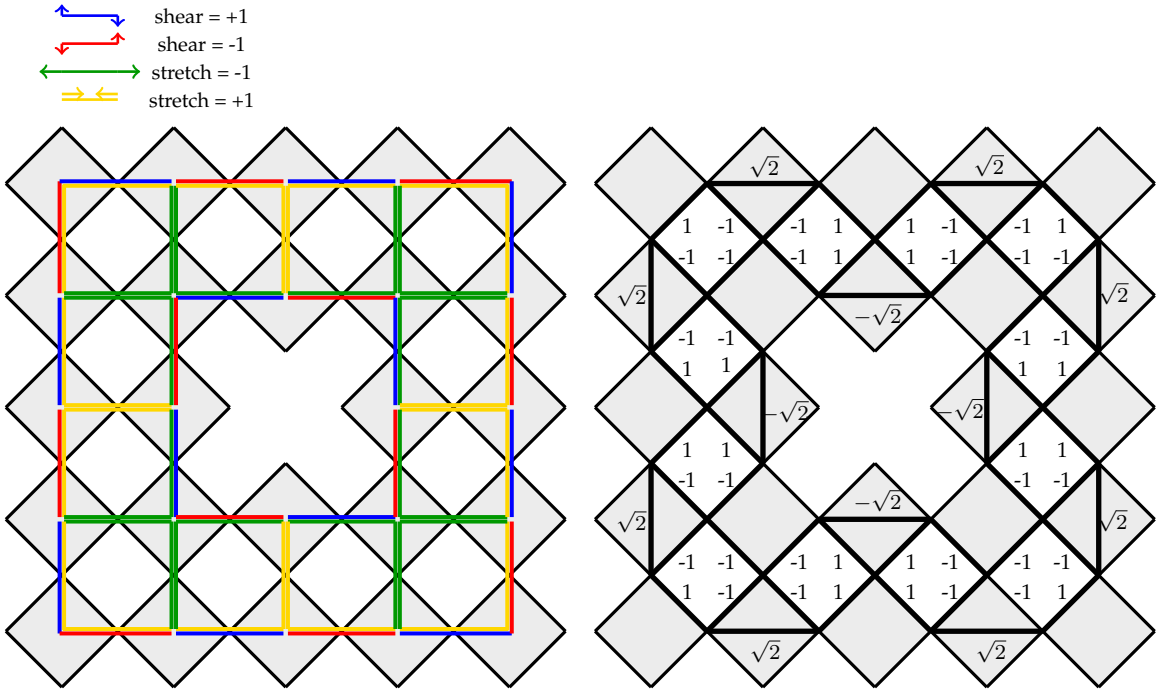

(a) First state of selfstress in representation [a]. (b) First state of selfstress in representation [b].

Figure 3.16: The first state of selfstress for a tiling of size 5×5, with the centre tiling removed.

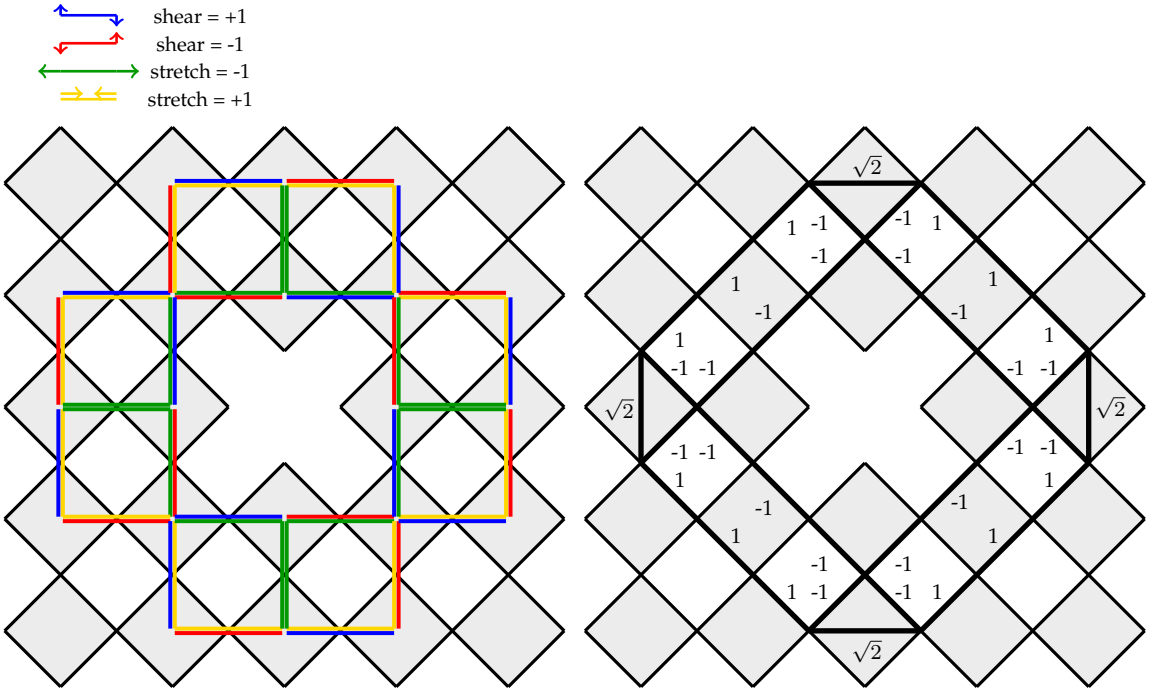

(a) Second state of selfstress in representation [a]. (b) Second state of selfstress in representation [b].

Figure 3.17: The second state of selfstress.

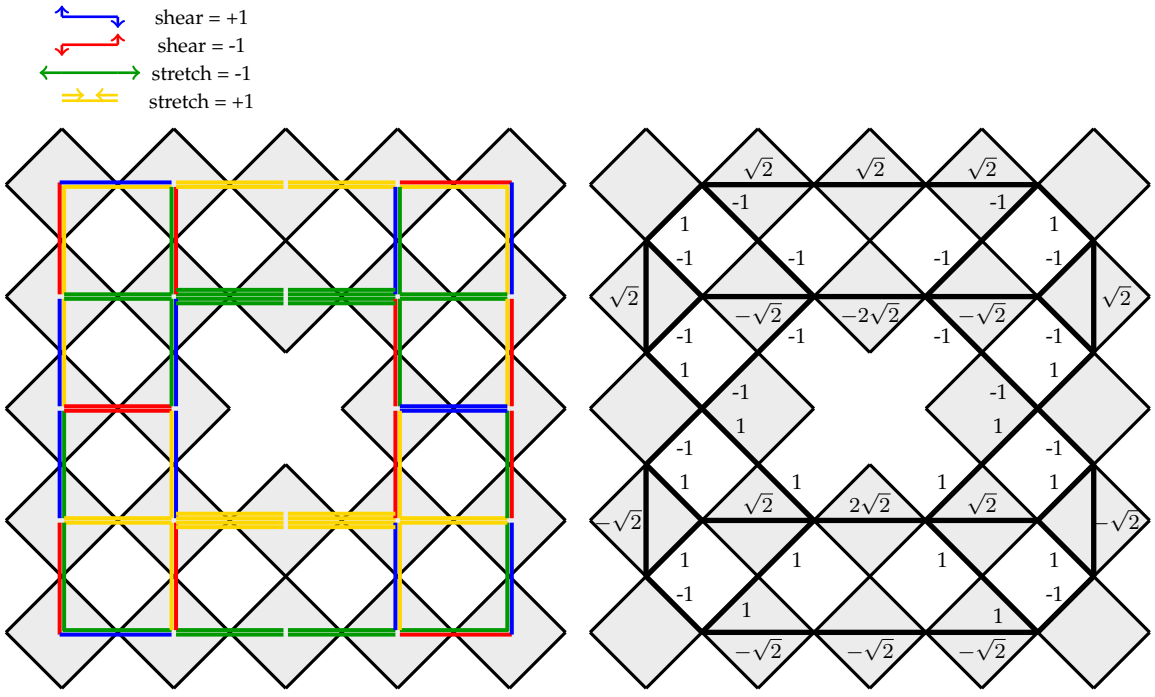

(a) Third state of selfstress in representation [a]. (b) Third state of selfstress in representation [b].

Figure 3.18: The third state of selfstress.

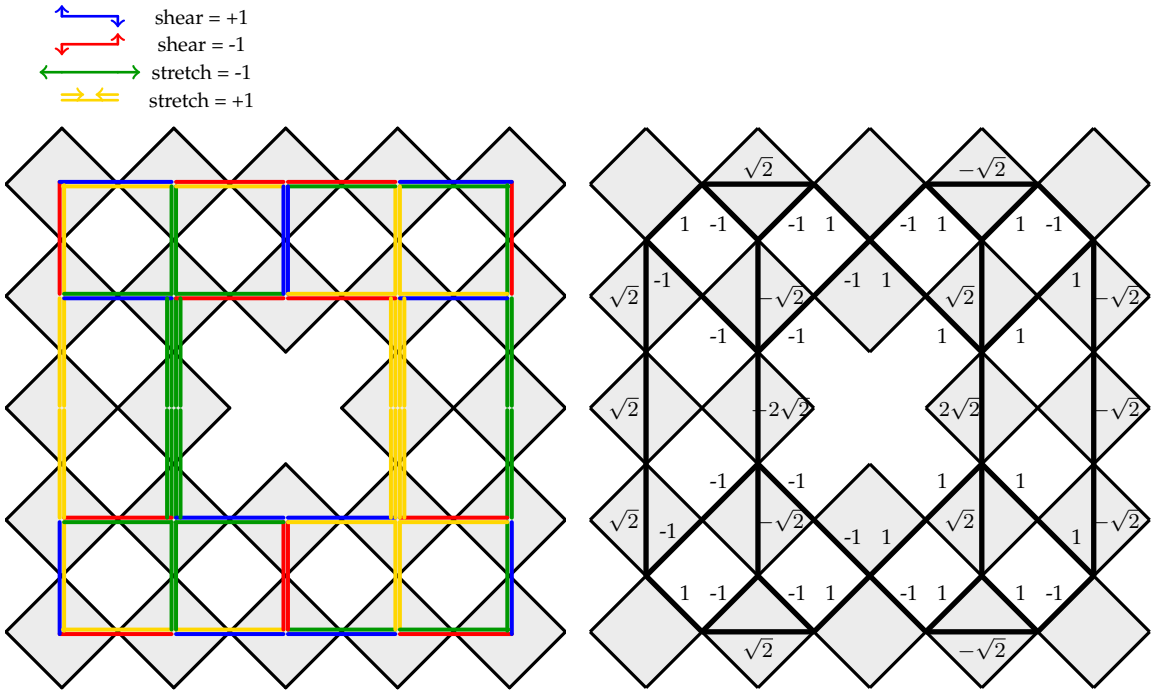

(a) Fourth state of selfstress in representation [a]. (b) Fourth state of selfstress in representation [b].

Figure 3.19: The fourth state of selfstress.

Because of the explanation in Section 3.3, these above states of selfstress can be constructed by using the independent local 3×3 states. There exists a systematic approach to construct the larger states of selfstress, using local 3×3 states, by using the fact that in the holes, the forces from the 3×3 subtilings have to cancel out. To use this approach, we have to choose one of the representations. For representation [a], the forces on the bonds as defined in Figure 3.1 are easy to be working with, and thus we will use representation [a] to construct the states of selfstress.

In general, let us assume that there are N independent 3×3 states of selfstress in the tiling with the tiles in the holes placed back. The column vector $\vec{\sigma}_j$ represents the stress on the tiling, due to the j-th 3×3 state of selfstress. This vector has a length equal to twice the amount of bonds in the complete tiling when the tiles in the holes are returned, for each bond a stretching and a shearing component. Since the holes are filled up, this implies that the vector has to contain all bonds that have a stress coming from one of the 3×3 states of selfstress on them. For any $n \times m$ tiling, this amount equals $2(n \cdot (m-1) + (n-1) \cdot m)$.

First of all, we will consider $\sigma_{kl,a,j}$ and $\sigma_{kl,s,j}$. These elements have the following interpretation: $\sigma_{kl,a,j} = 0$ and $\sigma_{kl,s,j} = 0$ respectively, if the bond between nodes k and l does not have an axial and shearing stress on the bonds, respectively, coming from the j-th state of selfstress. Similarly, $\sigma_{kl,a,j} \neq 0$ and $\sigma_{kl,s,j} \neq 0$ if there is an axial and shearing stress, respectively from the j-th state of selfstress on the bond between nodes k and l. Addition of a linear combination of the components of multiple states of selfstress, then gives:

$$\vec{\sigma}_{kl} = \begin{pmatrix} \sigma_{kl,a} \\ \sigma_{kl,s} \end{pmatrix} = \sum_{j=1}^{N} c_j \begin{pmatrix} \sigma_{kl,a,j} \\ \sigma_{kl,s,j} \end{pmatrix} = \sum_{j=1}^{N} c_j \vec{\sigma}_{kl,j}. \tag{3.3}$$

This gives a vector with two elements, for both the axial and shearing forces on the bond between k and l, due to a combination of the N covering states of selfstress.

Taking together all components of Equation 3.3, we get:

$$\vec{\sigma} = \begin{pmatrix} \vdots \\ \sigma_{kl,a} \\ \sigma_{kl,s} \\ \vdots \\ \sigma_{pq,a} \\ \sigma_{pq,s} \\ \vdots \\ \sigma_{rt,a} \\ \sigma_{rt,s} \\ \vdots \end{pmatrix} = \sum_{j=1}^{N} c_j \vec{\sigma}_j.$$

Here, $\vec{\sigma}_j$ is the j-th local 3×3 state of selfstress, and kl, pq and rt are different bonds between pairs of nodes.

Note that the bonds that are absent in the original system need to have a stress equal to 0 on them. Since all other bonds can have any combination of forces resulting from the covering states of selfstress, the only interesting part of this vector are these zero elements. Using this fact, we will consider a new vector $\vec{\sigma}_{|S}$, restricting the vector to the elements corresponding to the removed bonds. This implies that there should exist constants c_j, for $j = 1, 2, ..., N$, such that

$$\sigma_{|S} = \begin{pmatrix} 0 \\ 0 \\ \vdots \\ 0 \\ 0 \\ \vdots \\ 0 \\ 0 \end{pmatrix} = \sum_{j=1}^{N} c_j \vec{\sigma}_{j|S},$$

where S is the collection of removed bonds. If we determine the different stresses of the local states of selfstress on the locations of the removed bonds, we can in this way determine the values of c_j, such that the stress on the bonds in S is zero. This can easily be done by combining the different columns of $\vec{\sigma}_{j|S}$, the vector $\vec{\sigma}_j$ corresponding to the j^{th} state of selfstress restricted to the removed bonds, in a matrix A and determine the nullspace of this matrix. The number of states of selfstress thus equals the dimension of the nullspace of the matrix A.

The states of selfstress for any general tiling can be calculated with Algorithm 1.

Algorithm 1 Algorithm to determine the linear independent states of selfstress of a general tiling, with holes.

1: **Step 1.** Let $T = \{$ set of removed tiles$\}$ and $S = \{$ the set of removed bonds$\}$. Temporarily place the tiles in T back into the tiling and number all 3×3 subtilings in this tiling $1, 2, ..., N$.
2: **Step 2.**
3: **for** j in $1, ..., N$ **do**
4: **for** k in S **do**
5: Determine $\vec{\sigma}_{k,j} = \begin{pmatrix} \sigma_{k,a,j} \\ \sigma_{k,s,j} \end{pmatrix}$
▷ The stresses due to the local 3×3 states for each removed bond.
6: **end for**
7: Construct $\vec{\sigma}_j$, by concatenation of the $\vec{\sigma}_{k,j}$. ▷ This gives a vector of length $2|S|$.
8: **end for**
9: Construct a matrix A, with in column j the vector $\vec{\sigma}_j$, for all $j \in \{1, 2, ..., N\}$.
▷ This matrix has size $2|S| \times N$.
10: **Step 3.** The nullspace of the matrix A gives all combinations c_i of possible linear independent states of selfstress for the tiling with holes. In this way, there are no forces over the removed bonds.

Theorem 3.5.2. Algorithm 1 is correct, and the calculation of the matrix A has complexity $O(|S| \cdot N)$, (instead of $O(3 \cdot \#$ of bonds in tiling$) \times (2 \cdot \#$ of bonds in tiling), for the computation of the matrix where the forces on all nodes have to be zero.)

Proof. The proof of this theorem follows from the construction of the matrix A, as explained above the algorithm. The above algorithm reduces the complexity of the calculation of the states of selfstress, from computing all combinations of forces on all bonds of the tiling, so that the net forces on the nodes is zero, to the calculation of a combination of forces due to the 3×3 states of selfstress on the removed bonds, so that the net force on all removed bonds is zero. This implies that the matrix size of which we need to determine the nullspace decreases from $(3 \cdot \#$ of bonds in tiling$) \times (2 \cdot \#$ of bonds in tiling), as defined for the transposed rigidity matrix in Section 2.2 to $2 \cdot |S| \times N$, where $|S|$ is the number of removed bonds and N the amount of local 3×3 states of selfstress. Thus the calculation of the matrix A is of order $O(|S| \times N)$. This reduction improves the calculation drastically, especially when only a few squares are removed. □

The resulting nullspace of this matrix A will give vectors corresponding to the states of selfstress. We will use this approach to determine the states of selfstress of different sorts of tilings, all containing holes.

Example 3.5.1 (Continued)**.** Consider the configuration in Example 3.5.1. The bonds between the squares can be numbered as in Figure 3.20.

Note that from Figure 3.20 we see that of these 40 bonds 36 are still present, and four of the bonds have been removed, namely: $S = \{16, 20, 21, 25\}$.

The nine local states of selfstress in the system can be numbered as depicted in Figure 3.21.

For each of the four removed bonds the forces of all nine local 3×3 states of selfstress can be determined. All nine states of selfstress contain edges over removed bonds of the tiling. Note that to have a state of selfstress, that is zero over the removed bonds of the tiling, we

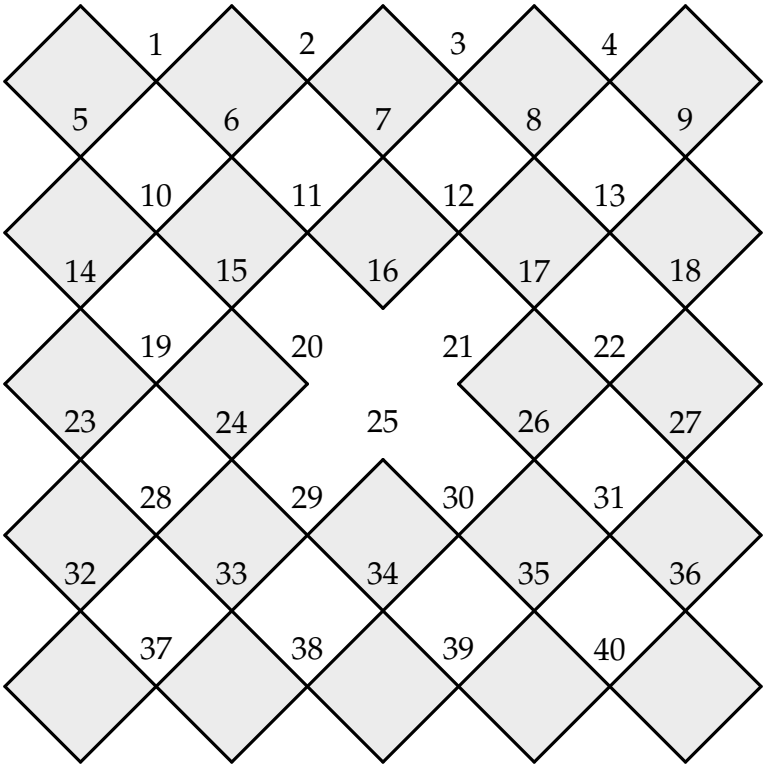

Figure 3.20: Numbering of the bonds between the squares of the 5×5 with a hole in the center. The bonds $S = \{16, 20, 21, 25\}$ are removed, because the square in the center has been taken out of the tiling.

have to add one or more of the nine possible states of selfstress. Consider the local state of selfstress 1, depicted in yellow in Figure 3.21.

This first local state of selfstress only concerns the removed bonds 16 and 20. After comparison with Figures 3.7a and 3.1, this implies: $\sigma_{16,1} = \begin{pmatrix} 1 \\ -1 \end{pmatrix}$, $\sigma_{20,1} = \begin{pmatrix} 1 \\ 1 \end{pmatrix}$, $\sigma_{21,1} = \begin{pmatrix} 0 \\ 0 \end{pmatrix}$ and $\sigma_{25,1} = \begin{pmatrix} 0 \\ 0 \end{pmatrix}$, giving

$$\sigma_{1|S} = \begin{pmatrix} 1 \\ -1 \\ 1 \\ 1 \\ 0 \\ 0 \\ 0 \\ 0 \end{pmatrix}.$$

In the same way, we can also find the vectors corresponding to all other local states of selfstress:

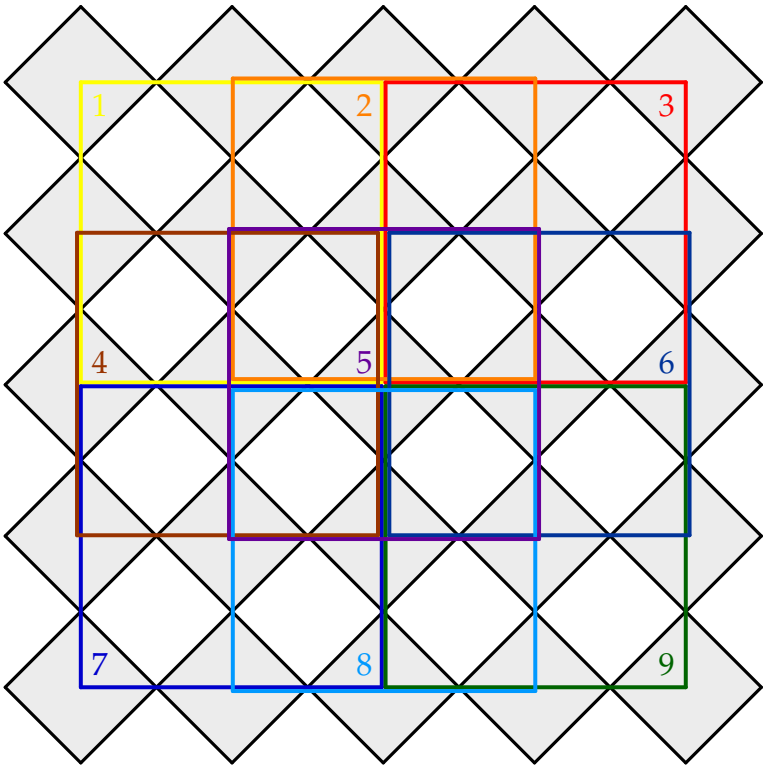

Figure 3.21: The different local states of stelfstress in a 5×5 system. Here $N = 9$.

$$\sigma_{2|S} = \begin{pmatrix} -2 \\ 0 \\ 1 \\ -1 \\ 1 \\ 1 \\ 0 \\ 0 \end{pmatrix}, \sigma_{3|S} = \begin{pmatrix} 1 \\ 1 \\ 0 \\ 0 \\ 1 \\ -1 \\ 0 \\ 0 \end{pmatrix}, \sigma_{4|S} = \begin{pmatrix} 1 \\ 1 \\ -2 \\ 0 \\ 0 \\ 0 \\ 1 \\ -1 \end{pmatrix}, \sigma_{5|S} = \begin{pmatrix} -2 \\ 0 \\ -2 \\ 0 \\ -2 \\ 0 \\ -2 \\ 0 \end{pmatrix}, \tag{3.4}$$

$$\sigma_{6|S} = \begin{pmatrix} 1 \\ -1 \\ 0 \\ 0 \\ -2 \\ 0 \\ 1 \\ 1 \end{pmatrix}, \sigma_{7|S} = \begin{pmatrix} 0 \\ 0 \\ 1 \\ -1 \\ 0 \\ 0 \\ 1 \\ 1 \end{pmatrix}, \sigma_{8|S} = \begin{pmatrix} 0 \\ 0 \\ 1 \\ 1 \\ 1 \\ -1 \\ -2 \\ 0 \end{pmatrix}, \sigma_{9,S} = \begin{pmatrix} 0 \\ 0 \\ 0 \\ 0 \\ 1 \\ 1 \\ 1 \\ -1 \end{pmatrix}.$$

By Theorem 3.5.2, we need: $\vec{0} = \sum_{j=1}^{9} c_j \sigma_{j|S}$, in other words, we need to solve:

$$\begin{pmatrix}0\\0\\0\\0\\0\\0\\0\\0\end{pmatrix} = \begin{pmatrix}1&-2&1&1&-2&1&0&0&0\\-1&0&1&1&0&-1&0&0&0\\1&1&0&-2&-2&0&1&1&0\\1&-1&0&0&0&0&-1&1&0\\0&1&1&0&-2&-2&0&1&1\\0&1&-1&0&0&0&0&-1&1\\0&0&0&1&-2&1&1&-2&1\\0&0&0&-1&0&1&1&0&-1\end{pmatrix}\begin{pmatrix}c_1\\c_2\\c_3\\c_4\\c_5\\c_6\\c_7\\c_8\\c_9\end{pmatrix}. \tag{3.5}$$

This is equivalent to finding the nullspace of this matrix. Using Python, we find the following basis of the nullspace:

$$\vec{c}_1 = \begin{pmatrix}1\\0\\1\\0\\1\\0\\1\\0\\1\end{pmatrix}, \vec{c}_2 = \begin{pmatrix}0\\1\\0\\1\\0\\1\\0\\1\\0\end{pmatrix}, \vec{c}_3 = \begin{pmatrix}1\\0\\3\\1\\2\\3\\1\\2\\3\end{pmatrix}, \vec{c}_4 = \begin{pmatrix}1\\1\\1\\2\\2\\2\\3\\3\\3\end{pmatrix}.$$

As a convenient visualisation, corresponding to Figure 3.21, we rewrite the basis in terms of 3×3 states of selfstress:

$$\vec{c}_1 = \begin{bmatrix}1&0&1\\0&1&0\\1&0&1\end{bmatrix}, \vec{c}_2 = \begin{bmatrix}0&1&0\\1&0&1\\0&1&0\end{bmatrix}, \vec{c}_3 = \begin{bmatrix}1&1&1\\0&0&0\\-1&-1&-1\end{bmatrix}, \vec{c}_4 = \begin{bmatrix}1&0&-1\\1&0&-1\\1&0&-1\end{bmatrix},$$

which correspond to the configurations defined in Figures 3.16-3.19. In these 3×3 states of selfstress, the element (i, j) in row i and column j corresponds to the size of the basis state of selfstress on the place of the (i, j)-th 3×3 subtiling.

Since we know that any state of selfstress on a 3×3 tiling can be written as a linear combination of these four states of selfstress, we can also change the used basis states of selfstress to the following, more structured representation:

$$\vec{c}_1 = \begin{bmatrix}1&0&1\\0&1&0\\1&0&1\end{bmatrix}, \vec{c}_2 = \begin{bmatrix}0&1&0\\1&0&1\\0&1&0\end{bmatrix}, \vec{c}_3 = \begin{bmatrix}0&0&0\\1&1&1\\2&2&2\end{bmatrix}, \vec{c}_4 = \begin{bmatrix}0&1&2\\0&1&2\\0&1&2\end{bmatrix}$$

There are always two squares between the hole and the outer boundary in Example 3.5.1. This implies that there are no zero modes apart from the three translational modes and the trivial hinging mode. This is immediate since there are no squares that can move independently of other squares. We will show that every tiling with two squares between the boundaries everywhere, has four states of selfstress.

Theorem 3.5.3. Any $n \times m$ tiling with only one hole of size $(n-4) \times (m-4)$ in its centre, for which there are at least two squares between the boundary enclosing the hole in the tiling,

and the outer boundary, has 4 states of selfstress. These can be written as:

$$\vec{c}_1 = \begin{bmatrix} 1 & 0 & 1 & 0 & \dots \\ 0 & 1 & 0 & 1 & \dots \\ 1 & 0 & 1 & 0 & \dots \\ 0 & 1 & 0 & 1 & \dots \\ \vdots & \vdots & \vdots & \vdots & \ddots \end{bmatrix}, \vec{c}_2 = \begin{bmatrix} 0 & 1 & 0 & 1 & \dots \\ 1 & 0 & 1 & 0 & \dots \\ 0 & 1 & 0 & 1 & \dots \\ 1 & 0 & 1 & 0 & \dots \\ \vdots & \vdots & \vdots & \vdots & \ddots \end{bmatrix},$$

$$\vec{c}_3 = \begin{bmatrix} 0 & 1 & 2 & 3 & \dots \\ 0 & 1 & 2 & 3 & \dots \\ 0 & 1 & 2 & 3 & \dots \\ 0 & 1 & 2 & 3 & \dots \\ \vdots & \vdots & \vdots & \vdots & \ddots \end{bmatrix}, \vec{c}_4 = \begin{bmatrix} 0 & 0 & 0 & 0 & \dots \\ 1 & 1 & 1 & 1 & \dots \\ 2 & 2 & 2 & 2 & \dots \\ 3 & 3 & 3 & 3 & \dots \\ \vdots & \vdots & \vdots & \vdots & \ddots \end{bmatrix}.$$

Proof. In general, for any $n \times m$ tiling with a $(n-4) \times (m-4)$ hole in the center, we have $4 \cdot 4 + 4 \cdot (m-4) + 4 \cdot (n-4) = 4n + 4m - 16$ squares. There are $4 \cdot (m-1) + 2 \cdot (n-4)$ horizontal bonds and $4 \cdot (n-1) + 2 \cdot (m-4)$ vertical ones, which gives $n_{CON} = 2 \cdot (4 \cdot (m-1) + 2 \cdot (n-4) + 4 \cdot (n-1) + 2 \cdot (m-4)) = 12n + 12m - 48$. Thus $n_{CON} - n_{DOF} = 12n + 12m - 48 - 3 \cdot (4n + 4m - 16) = 0$.

Since the system does not have any local zero modes, the only zero modes are the global ones, and thus: $n_{SSS} - 4 = n_{SSS} - n_{ZM} = n_{CON} - n_{DOF} = 0$, so that $n_{SSS} = 4$.

By plugging the states of selfstress $\vec{c}_1, \vec{c}_2, \vec{c}_3$ and $\vec{c}_4$ in the tilings, it is easy to deduce that these states of selfstress are correct. Namely, when doing so, all forces on the edges within the hole cancel out and the only remaining stresses are the ones in the two outer boundaries.

These four elements are linearly independent. Thus, we obtain that these four form a basis for the states of selfstress in any $n \times m$ tiling, with a $(n-4) \times (m-4)$ hole in the center. □

In the case that the hole in the tiling is smaller, more states of selfstress will appear. In general, it is always possible to determine the states of selfstress with the above strategy.

3.6 States of selfstress in tilings with holes: examples

We have seen in Section 3.5 that we can use Algorithm 1 to find the linear independent states of selfstress of a tiling. In this section, we will show the results for multiple examples.

Example 3.6.1. Consider the tiling in Figure 3.22, with the single state of selfstress corresponding to this tiling depicted in the figure. This is the same tiling as depicted in Figure 3.13, but in this tiling the squares without forces contributing to the state of selfstress are removed. This tiling is interesting, because on one of the sides of the hole, the tiling has only one square, all over this side.

This configuration gives the nullspace: $\vec{c} = \begin{bmatrix} 1 & 2 \\ 1 & 2 \\ 1 & 2 \end{bmatrix}$. Note that we can also consider equivalent tilings with a bigger hole, and thus there are more removed squares. One example of this is depicted in Figure 3.23.

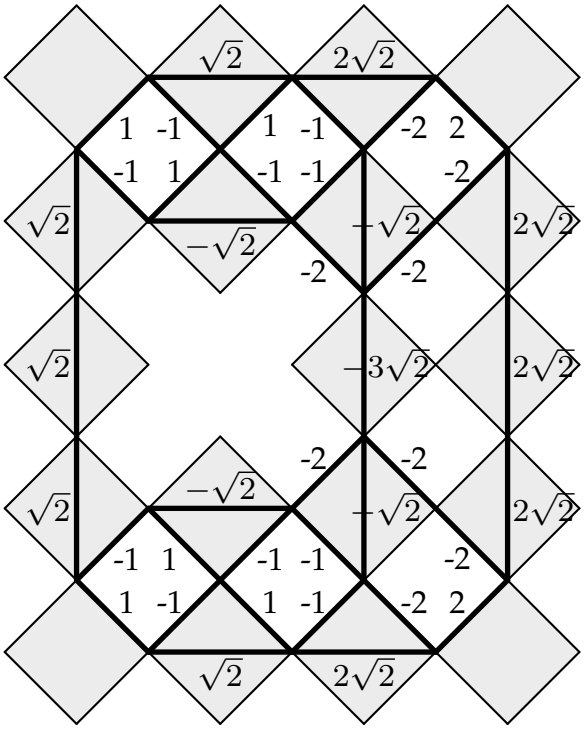

Figure 3.22: 5×4 tiling with one removed square, in which on one side of the hole, there is only one row of squares. In this tiling there is one state of selfstress.

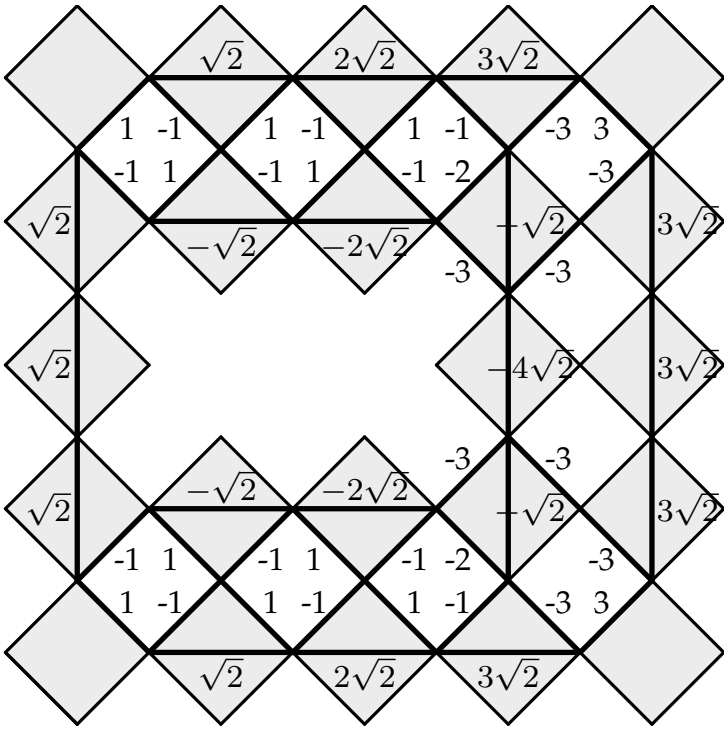

Figure 3.23: A 5×5 tiling, with a 1×2 hole. For this tiling, there also is one state of selfstress.

The nullspace corresponding to the tiling in Figure 3.23 is $\vec{c} = \begin{bmatrix} 1 & 2 & 3 \\ 1 & 2 & 3 \\ 1 & 2 & 3 \end{bmatrix}$. In an equivalent

way, the tiling can be extended to any tiling with more rows and columns of squares, with a width of one square on one side, and that has a width of two squares on the other sides of the hole, where these states of selfstress can be written as: $\vec{c} = \begin{bmatrix} 1 & 2 & 3 & \dots \\ 1 & 2 & 3 & \dots \\ 1 & 2 & 3 & \dots \\ \vdots & \vdots & \vdots & \ddots \end{bmatrix}$

The tilings in Figures 3.16-3.19 are the basis tilings that can be positioned around a single hole. Any other tiling, around any single hole, can be written as a linear combination of these tilings and any combination of 3×3 states of selfstress. Figure 3.24 gives an example of a tiling that is a combination of a variant of the tiling in Figure 3.22 and a 3×3 state of selfstress.

Example 3.6.2. Consider the tiling depicted in Figure 3.24. The nullspace of this tiling has a representation in the local 3×3 states of selfstress, given by: $\vec{c} = \begin{bmatrix} 0 & 1 & 1 & 1 \\ 2 & 2 & 2 & 2 \\ 3 & 3 & 3 & 3 \\ 4 & 4 & 4 & 4 \end{bmatrix}$. Note that this tiling is equivalent to an extended, rotated version of the tiling in Figure 3.22, but in which the tile in the upper left corner is removed, and two additional tiles are added, so that subtraction of the local 3×3 state of selfstress in the upper left corner, compared to the extended version, results in a feasible selfstress on the entire tiling.

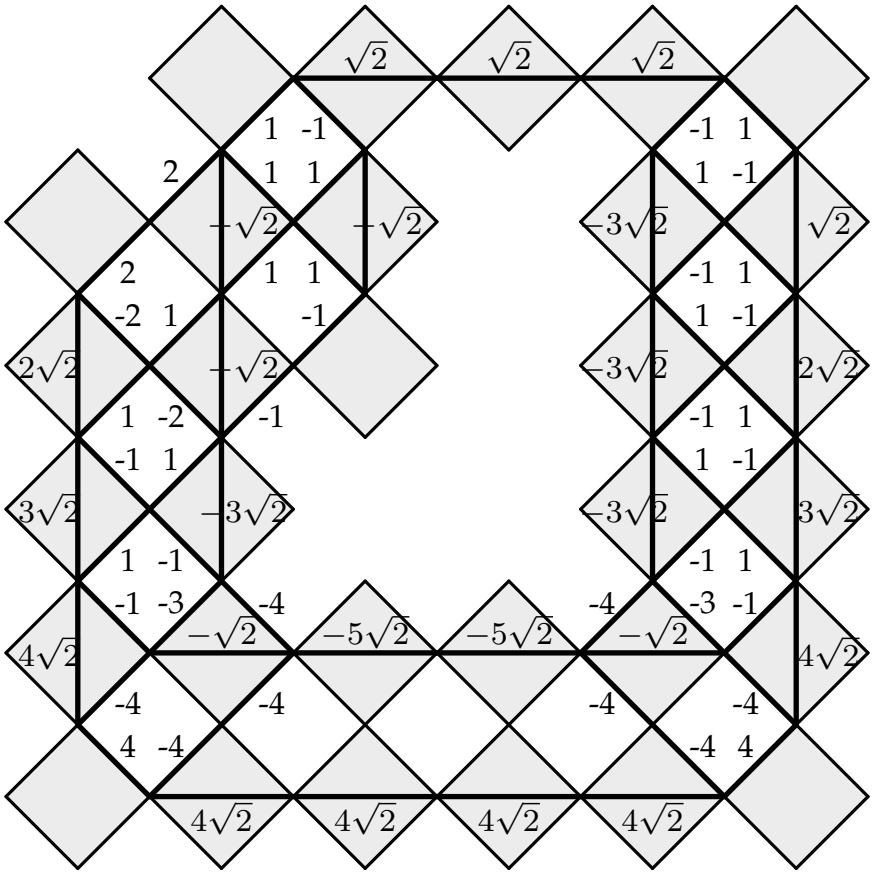

Figure 3.24: A tiling for which we have a combination of a larger variant of the tiling in Figure 3.22 and a 3×3 tiling.

We will consider two more examples, two so-called dilution examples from the PhD thesis of L.A. Lubbers [6]. These tilings both consist of multiple clusters of squares, with a couple of single bonds between them. In the first example, see Figure 3.25a, these bonds are placed in such a way that there still is just one local zero mode in the system. In the second example, see Figure 3.25b, the connections between the clusters do not constrain all motions of the independent clusters in the tiling, so that there is more than one zero mode.

For the first example in Figure 3.25, we find: $N = 47$, $B = 42$ and $n_{ZM} = 4$, so that, with: $n_{SSS} = N - B + n_{ZM} = 47 - 42 + 4 = 9$. We can easily see, that there are the 8 independent 3×3 states of selfstress in the lower cluster of the tiling. Thus there is one state of selfstress, that remains to be found. We see, that none of the already treated states of selfstress fit inside the above tiling, from which follows that we have to find a new state of selfstress.

For the second example, we find: $N = 60$, $B = 44$ and $n_{ZM} = 6$, since there are three local zero modes: the two independent hinging modes and the shearing between the components. Thus, we have $n_{SSS} = N - B + n_{ZM} = 60 - 44 + 6 = 22$. It is easy to see, that on both sides of the single bonds, we have 10 3×3 states of selfstress, from which follows that there remain 2 other states of selfstress to be found.

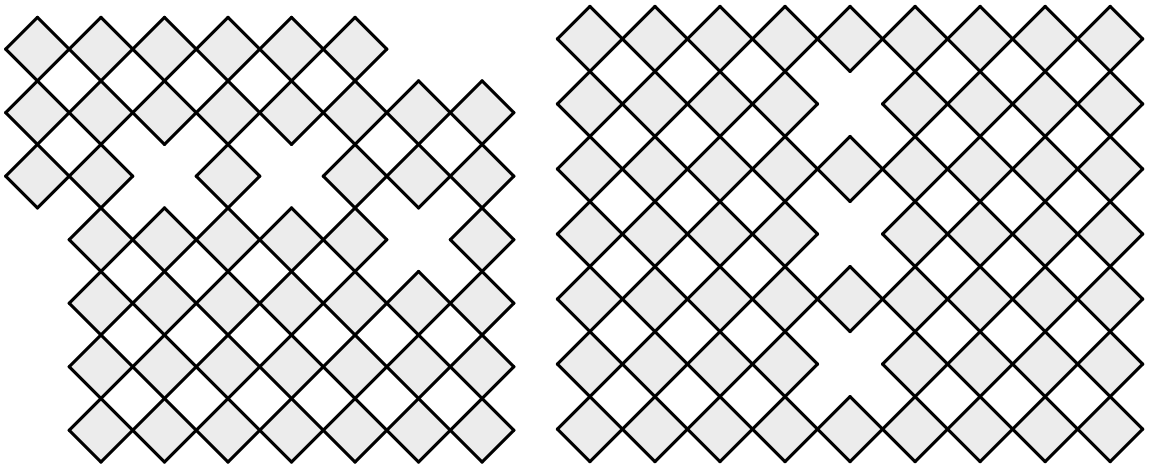

(a) The first example of a tiling consisting of multiple clusters. In this example, there is only one local zero mode: the shearing of the total system. This tiling has 9 states of selfstress, of which there are 8 3×3 states of selfstress.

(b) The second example with multiple clusters. In this example, there are three zero modes: the two independent hinging modes of the two components, and the shear of one of the components, with respect to the other. Thus, this tiling has 22 states of selfstress, of which there are 20 3×3 states of selfstress.

Figure 3.25: Tilings consisting of multiple clusters, that have additional states of selfstress, apart from the 3×3 state of selfstress. The other states of selfstress in these tilings are of the form depicted in 3.26.

In both tilings, the missing states of selfstress are the same. This state of selfstress is also on a tiling of size 5×5, with holes at $(2, 3)$ and at $(4, 3)$ and is depicted in Figure 3.26. The corresponding 3×3 representation is:

$$\vec{c} = \begin{bmatrix} 1 & 1 & 1 \\ 2 & 2 & 2 \\ 1 & 1 & 1 \end{bmatrix}.$$

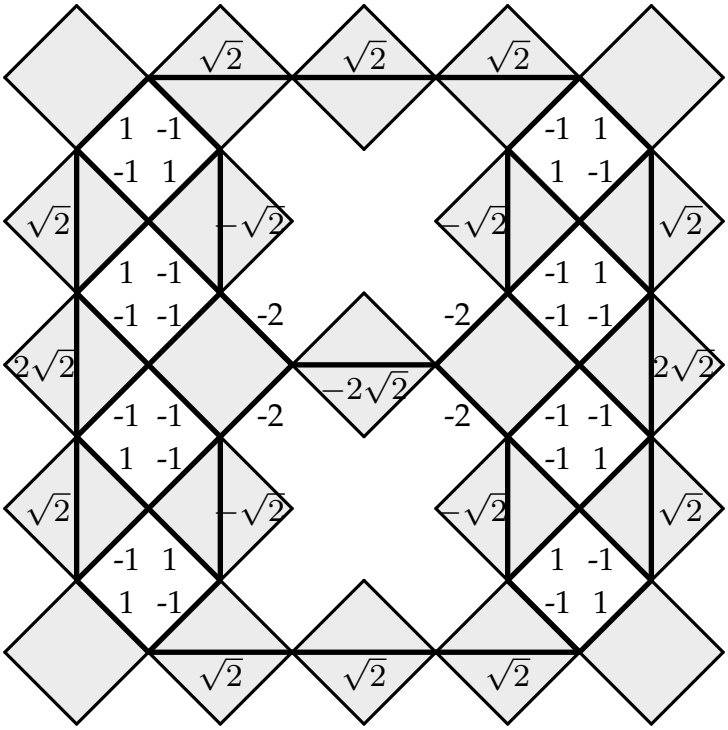

Figure 3.26: The state of selfstress that is found in both tilings of Figure 3.25.

Plugging these back in the example, the states of selfstress are located in the tilings as depicted in Figure 3.27. For simplicity, we have not depicted the full states of selfstress, but only indicated, which tiles have non-zero forces due to these states of selfstress.

Again, this state of selfstress can be extended to a tiling with bigger holes. This is for example depicted in Figure 3.28, where the state of selfstress is a combination of the states of selfstress in Figures 3.22 and 3.26. The state of selfstress in Figure 3.28 has a corresponding 3×3-representation:

$$\vec{c} = \begin{bmatrix} 2 & 2 & 2 \\ 4 & 4 & 4 \\ 6 & 6 & 6 \\ 3 & 3 & 3 \end{bmatrix},$$

which is a linear combination of the state of selfstress in Figure 3.22, rotated over 90°:

$$\vec{c_1} = \begin{bmatrix} 2 & 2 & 2 \\ 1 & 1 & 1 \\ 0 & 0 & 0 \\ 0 & 0 & 0 \end{bmatrix} \tag{3.6}$$

and the state of selfstress in Figure 3.26:

$$\vec{c_2} = 3 \begin{bmatrix} 0 & 0 & 0 \\ 1 & 1 & 1 \\ 2 & 2 & 2 \\ 1 & 1 & 1 \end{bmatrix}. \tag{3.7}$$

Of course, this approach can be extended even more, to make the tiling larger in the vertical direction, by adding the matrix from Equation 3.6 to the matrix of Equation 3.7 one or more

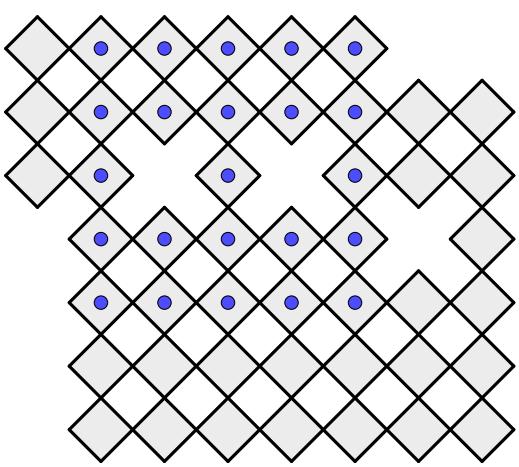

(a) In blue, we have indicated the non-3×3 state of selfstress of this tiling. The state of stelfstress is rotated over 90° with respect to the state of selfstress depicted in Figure 3.26.

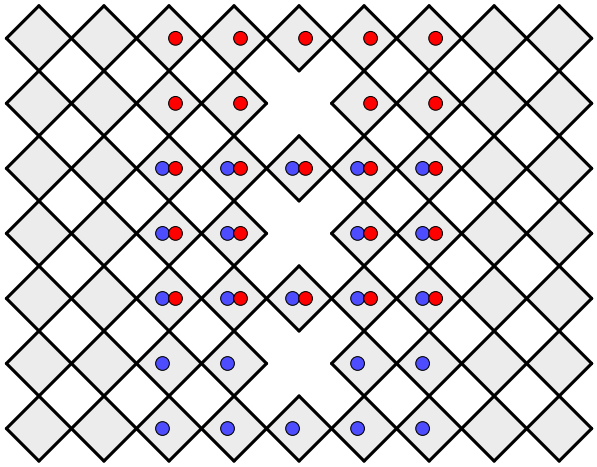

(b) In blue and red, the two non-3×3-states of selfstress are indicated. In this tiling, any linear combination of these two and the 3×3 states of selfstress in the tiling, will give a possible solution for a state of selfstress in the tiling.

Figure 3.27: The states of selfstress of the two examples that are not 3×3 states of selfstress. These are all cases of the state of selfstress depicted in Figure 3.26.

times. In the horizontal direction, the state of selfstress can be extended by adding another copy of the rows to the matrix of the 3×3 representation of the state of selfstress.

Up to now, we only have done all calculations for tilings in which tiles are removed. This can also be done for tilings in which not only tiles are missing, but also pairs of corners are not connected. In this case, the forces of the states of selfstress can no longer be located over the bonds between these squares. The bonds that are not connected in Algorithm 1, also have to be considered in the collection of S, when determining the states of selfstress. An example of this problem is given in Chapter 5.

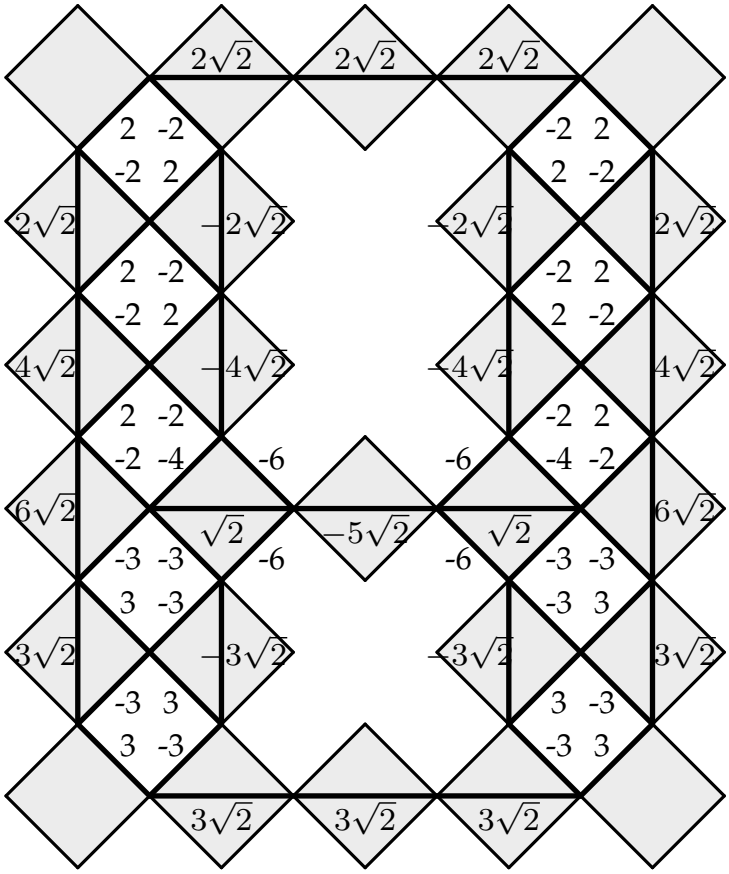

Figure 3.28: Extension of the state of selfstress in Figure 3.26.

Chapter 4

Creating holes: classifying the states of selfstress

In this chapter, we will consider the amount of states of selfstress and zero modes that both may disappear or appear in a tiling as a result of adding holes to the tiling. It is important to note, that in this section we will consider different $n \times m$ rectangular tilings. Any tiling can be embedded in this general $n \times m$ tiling and the states of selfstress on the original tiling can be written as a combination of the derived states of selfstress on more general tilings and 3×3 states of selfstress. Thus, from the rectangular tiling, we can create all tilings, and therefore these are sufficient to consider.

In the first section, we consider single holes, so tilings that have only one hole (of one tile or multiple neighbouring tiles). In Section 4.2, we will look at multiple holes, that are separated a distance of at least two tiles from each other, and thus any 3×3 state of selfstress covering parts of one hole does not cover parts of other holes. In Section 4.3 we consider holes in the tiling that are one tile apart, and have 3×3 states of selfstress covering these two holes in the tiling.

4.1 Single holes

4.1.1 Removal of a single tile in the tiling

In general, we will assume that the tiling is rectangular and with size $n \times m$, for $n, m \geq 3$. The reason that we can do this, is that there exists at least one state of selfstress in this tiling, so that removal of tiles influences at least one state of selfstress. First of all, we will assume that $n, m \geq 5$, for convenience, because in smaller tilings the created holes are equivalent to the problems discussed in Chapter 3. The example tiling we will be looking at, is depicted in Figure 4.1.

For the tiling in Figure 4.1, we will calculate the difference in the number of tiles, ΔN, (which will always be -1, if we remove one tile in the tiling), the difference in the number of corners lying on the polygon boundary, ΔB, (which is $+0$ if the removed tile is a corner of the tiling, $+2$ if the removed tile is on the boundary of the tiling, and $+4$ if the removed tile is located within the tiling). The Maxwell-Calladine equation also has to hold after a tile

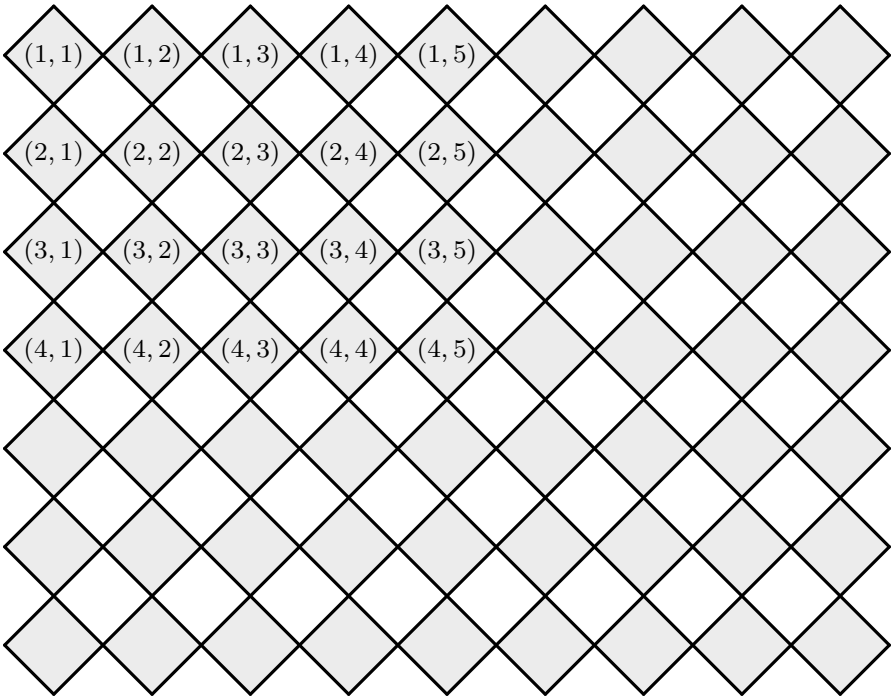

Figure 4.1: General (in this case 7×9) tiling. We consider what happens by removing certain tiles from the tiling, and what the effect is on the number of states of selfstress and zero modes. We consider this for the numbered tiles, removal of all other tiles is equivalent due to rotations of the tiling.

has been removed, and thus, using Equation 3.1:

$$(N + \Delta N) - (B + \Delta B) = (n_{SSS} + \Delta n_{SSS}) - (n_{ZM} + \Delta n_{ZM}), \tag{4.1}$$

where Δn_{SSS} the difference in the number of states of selfstress, and Δn_{ZM} the difference in the number of zero modes. Substracting Equation 3.1, gives:

$$\Delta N - \Delta B = \Delta n_{SSS} - \Delta n_{ZM}, \tag{4.2}$$

so that the difference between the number of states of selfstress and the number of zero modes is determined by the location of the removed tile within the tiling. In Table 4.1, the effect of the removal of specific tiles is illustrated, and in Figure 4.2, all removed squares with equal values of all parameters in Equation 4.2 are indicated in the same color.

From Table 4.1, it can be seen that we can classify the tiles depending on the numbers of states of selfstress and zero modes that change, and the kinds of states of selfstress that appear, when removing a tile. It follows that the difference $\Delta n_{SSS} - \Delta n_{ZM}$ is equal to

- -1, if the removed tile is a tile at the corner,
- -3 if the removed tiling is a boundary tile, but not a corner tile,
- -5 if the removed tile is not on the boundary.

On the other hand, there is a pattern in the removed number of states of selfstress in the tiling, depending on how close the removed tile is to the boundaries. This pattern is shown in Figure 4.2. For all tiles with a dot of the same color, the change in parameters is equal when these tiles are removed. By removal of a corner tile (red coloured), the boundary tiles

Removed square	ΔN	ΔB	$\Delta N - \Delta B$	Δn_{SSS}	Δn_{ZM}
$(1,1)$	-1	0	-1	-1	0
$(1,2),(2,1)$	-1	+2	-3	-2	+1
$(1,3),(1,4),(1,5),$ $(3,1),(4,1)$	-1	+2	-3	-3	0
$(2,2)$	-1	+4	-5	-4	+1
$(2,3),(2,4),(2,5),$ $(3,2),(4,2)$	-1	+4	-5	-5	0
$(3,3),(3,4),(3,5)$	-1	+4	-5	-5	0

Table 4.1: This table contains the difference in the number of tiles, ΔN, the difference in the number of boundary elements, ΔB, the difference in the number of states of selfstress, Δn_{SSS}, and the difference in the number of zero modes, Δn_{ZM}, for all tiles in the upper left quarter. The difference in the number of zero modes is easy to count in these configurations, just like the number of states of selfstress, as will be explained below.

(orange and yellow coloured), and tiles having a green color states of selfstress only disappear. Additionally, removal of all other tiles, i.e. the dark and light blue tiles, introduces new states of selfstress to the tiling. First of all, for the dark blue coloured tiles, six local 3×3 states of selfstress will disappear, but the state of selfstress of Figure 3.22 will reappear around the hole. For the light blue coloured tiles, the tiles in the bulk, nine states of selfstress will disappear, but the states of selfstress from Figures 3.16-3.19 will reappear around the hole.

For the green coloured tiling, a linear combination of the four 3×3 states of selfstress that cover the hole should result in a basic state of selfstress surrounding the hole, if there does exists a state of selfstress around this hole. Any non-zero linear combination of these four states of selfstress, as can be shown using the derivation of the matrix A in Algorithm 1, does not add up to zero at the removed tile, from which follows that no state of selfstress can appear in the tiling.

4.1.2 Decrease and increase in the number of states of selfstress due to one hole of multiple tiles

The decrease in the number of states of selfstress when one tile is removed, is equal to the number of disappearing local 3×3 subtilings, which is equal to

$$\alpha = (\text{vertical distance to the boundary} + 1)(\text{horizontal distance to the boundary} + 1).$$

This number is at most equal to 9, when a tile has a distance of at least two to both boundaries. When no states of selfstress can be formed out of covering states of selfstress surrounding the hole, and thus no state of selfstress appears, the total number of disappeared states of selfstress is equal to this number α. When states of selfstress appear in the tiling, so in the case that a light or dark blue dotted square is removed, the states of selfstress explained in Section 4.1.1 appear, and the change in the number of states of selfstress is equal to $\Delta n_{SSS} = \alpha + \{$ the number of appearing states of selfstress$\}$.

The above reasoning can also be applied to a tiling in which the hole is bigger, and thus

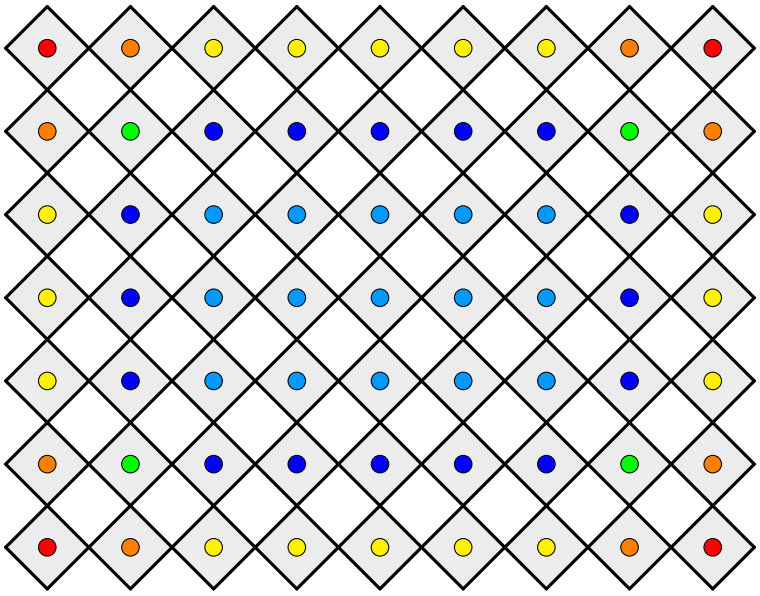

Figure 4.2: The different classifications of the tiles, when they are removed. All removed tiles with a dot of the same colour have the same change in parameters.

consisting of more tiles. In the case, that we have two neighbouring tiles that are removed, there are multiple options:

- The hole consisting of two tiles is located next to the boundary. This is because one of the two neighbouring tiles is located at the boundary, and the other is located next to this one, but not at the boundary. In total, we then have $\Delta B = 4$. Removal of the first tile, at the boundary, gives two additional boundary elements, and removal of the second tile inside the tiling gives another two.
- Both tiles are located at the boundary, and next to each other. In this case, we have $\Delta B = 2$. Removal of the first boundary element gives two additional boundary elements, but removal of the second tile does not give any additional boundary elements.
- Neither of the tiles is located at the boundary, but the tiles are next to each other. When this is the case, we have $\Delta B = 6$. In this case, we see for example that removal of the first tile gives four boundary elements, while removal of the second tile gives two additional boundary elements.

Both of the first two situations are specific cases of the tiling without holes explained in Section 3.4. In these situations, when the missing tiles are located at the boundary, we can easily determine the number of states of selfstress by counting the number of local 3×3 states of selfstress in the tiling.

In the case that the hole is not located at the boundary of the tiling, and we want to know what all possible states of selfstress in the tiling look like, we need to determine whether there exists a state of selfstress around the hole made in the tiling. Because we have assumed that the outer boundary of the tiling is a perfect rectangle, we only have to consider whether there exists a rectangular state of selfstress in the tiling around the hole. In general, the only square states of selfstress around one hole are comparable to the ones in Figures 3.16-3.19 and 3.22, but possibly with a larger hole. Thus the state of selfstress in the tiling surrounding the hole should look like one of these. The general solution to these problems can of course also be found by solving the linear system as derived in Algorithm 1. In Example 4.1.1 an

example of this is given.

Example 4.1.1. In this Figure 4.3 we find a 7×9 tiling with a hole in the inside of the tiling. We can determine that there are 5 states of selfstress in this tiling. For this tiling, the states of selfstress can be determined relatively easy. In this tiling, apart from the 3×3 states of selfstress, there also is the state of selfstress like the one in Figure 3.22, but with a larger hole.

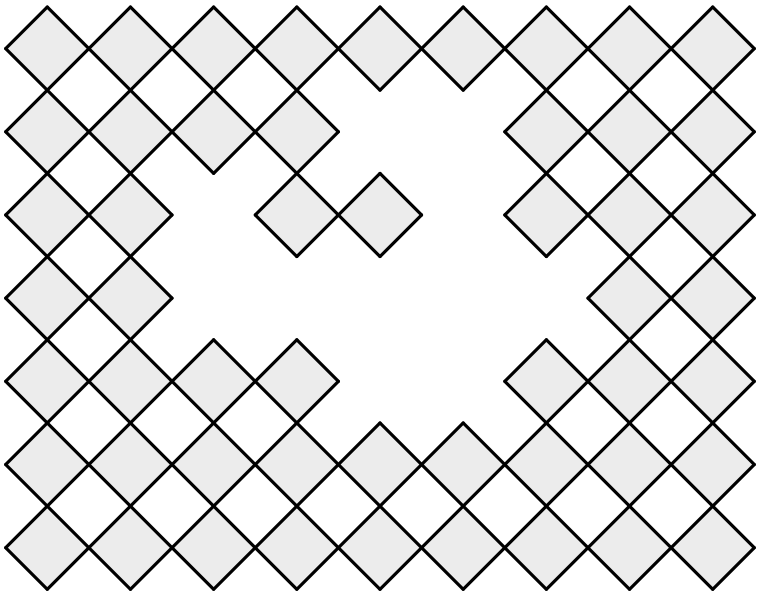

Figure 4.3: The 7×9 tiling with a general hole in the center. Here, $N = 52$, $B = 54$, $n_{ZM} = 7$, so $n_{SSS} = 5$, which are 4 local 3×3 states of selfstress, and one state of selfstress around the hole.

In the case that the tiling is not rectangular, it can be easy to see that states of selfstress are a linear combination of the tilings in Figures 3.16-3.19, 3.22 and the 3×3 subtilings. If this is not the case, it is always possible to find the states of selfstress using Algorithm 1.

4.2 Decomposing the tiling, holes at two or more tiles apart

In this section we will consider tilings for which the distance between different holes is more than two tiles wide. In this case, every covering 3×3 state of selfstress only covers one hole, because every other hole is not close enough to be covered by this state of selfstress. Thus, the problem of finding the states of selfstress of a large tiling can be decomposed into smaller tilings. These smaller tilings then only contain the states of selfstress that cover one hole and thus we can form linearly independent states of selfstress surrounding these single holes.

Of course, not all states of selfstress are surrounding one hole, but can also be surrounding multiple holes on a distance of one tile to each other. These holes can then be arranged into clusters of holes that are at a distance of one tile or less, and then the decomposition above can be applied if the distance between the different clusters is at least two tiles wide. Then we can find the states of selfstress on these decomposed tilings, surrounding the cluster and independent of the other clusters. The local 3×3 states of selfstress and these states of

selfstress on the decomposed tiling will give all possibilities for linearly independent states of selfstress in the tiling.

In the tilings we are looking for linearly independent states of selfstress. The combination of the independent states of selfstress surrounding holes and the 3×3 states of selfstress will give all independent combinations of the states of selfstress of the tiling. An example of this is given in Example 4.2.1.

Example 4.2.1. In Figure 4.4 an example of a tiling containing multiple states of selfstress is shown. In this example, the red and blue edges enclose the tiles that are contained in the 3×3 states of selfstress covering the holes, and thus the area in which the states of selfstress surrounding the holes have to be located. As a result, we can split up the tiling into two subtilings, consisting of the tiles enclosed by the boundaries, shown in Figure 4.5 on which we want to derive the states of selfstress surrounding the holes. Apart from the states of selfstress surrounding the holes, we have to find the local 3×3 states of selfstress in the complete tiling, and the combination of these local states of selfstress and the states of selfstress surrounding the holes give all independent states of selfstress in the tiling.

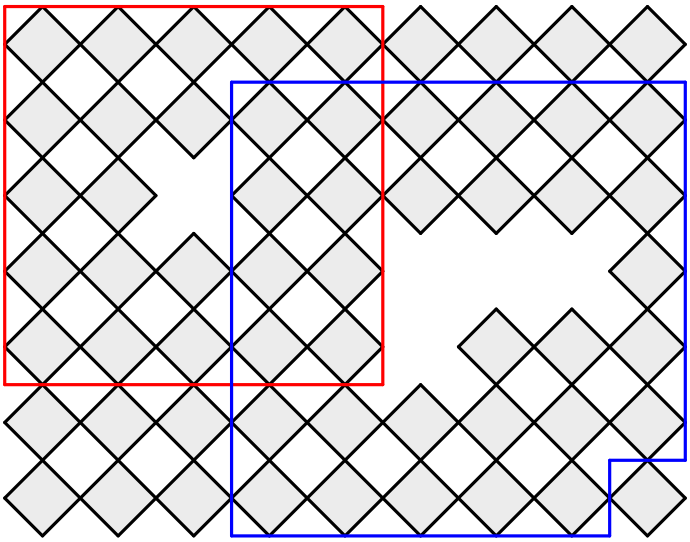

Figure 4.4: The 7×9 tiling with two holes, for which all 3×3 covering states of selfstress contain only (part of) one hole. The outer boundaries of these covering states of selfstress are depicted in red and blue, any state of selfstress surrounding the holes has to be located in these boundaries. Note that all 3×3 states of selfstress must be inside the tiling, and thus the blue boundary is constrained by the outside boundary of the tiling.

From the two subtilings in Figure 4.5, we see that the two holes have five linearly independent states of selfstress surrounding the holes, and since the two states of selfstress do not overlap, we know that these are the only ones surrounding the holes. Apart from these states of selfstress, the tiling also contains eleven 3×3 states of selfstress. In total, we thus can easily find the states of selfstress and detemine how many there are (which in this case is 16).

Of course, the above reasoning will also hold in the case that there are more holes at a distance of two or more tiles apart from all of the other holes in the tiling, as well as when there are a few holes that have an interference between the states of selfstress, while these holes are located in clusters that are at a distance of at least two tiles apart.

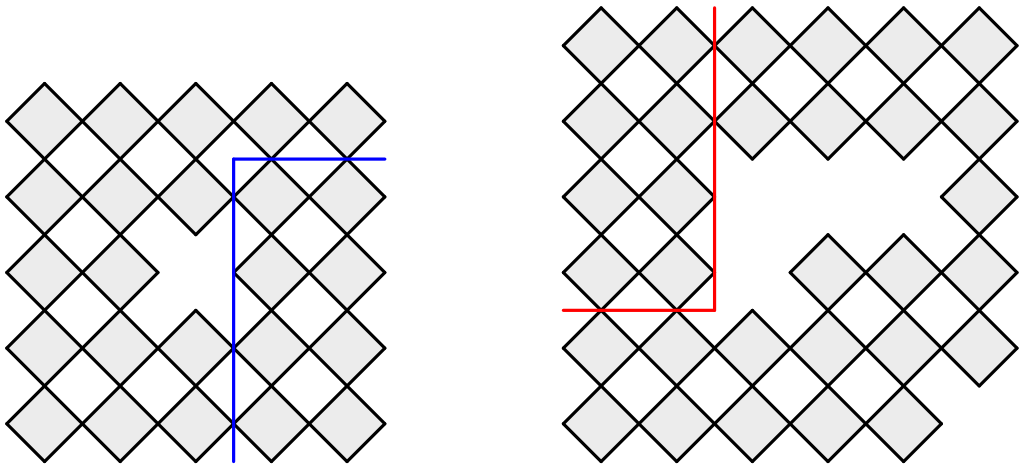

(a) The subtiling of the 7×9, surrounded by the red coloured boundary. This tiling is equivalent to the tiling described in Example 3.5.1 and thus the states of selfstress surrounding the holes are the states of selfstress depicted in Figures 3.16-3.19.

(b) The subtiling of the 7×9, surrounded by the blue coloured boundary. This tiling is equivalent to the tiling described in Example 3.6.2 and thus the state of selfstress surrounding the hole is the state of selfstress depicted in Figure 3.24.

Figure 4.5: The two subtilings on which states of selfstress surrounding the holes can appear.

4.3 Interference within tilings, holes at distances of one tile

When there is overlap between the states of selfstress surrounding the removed tiles, the situation becomes more complicated. For this case, we will give a few examples. We will again assume that we have the tiling from Figure 4.1. First consider the removal of the two tiles $(2, 2)$ and $(2, 4)$ from the tiling in Figure 4.1. This gives the tiling depicted in Figure 4.6.

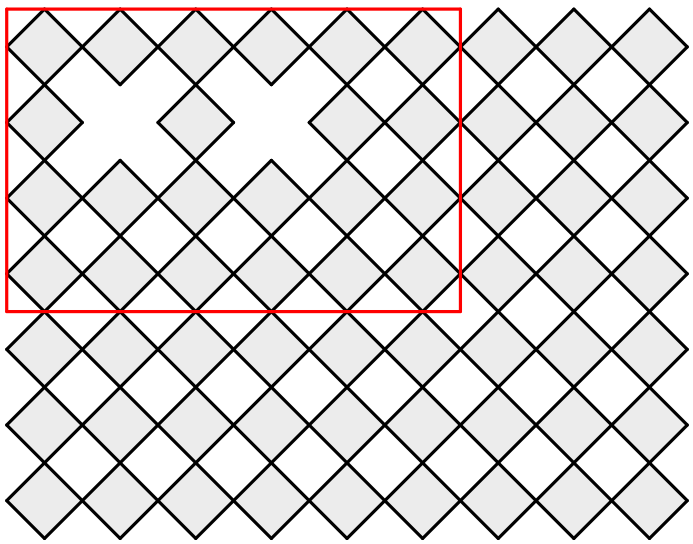

Figure 4.6: The 7×9 tiling with the tiles at $(2, 2)$ and $(2, 4)$ removed. All tiles that are covered by 3×3 states of selfstress over the holes are surrounded by the red boundary.

For the tiling depicted in Figure 4.6, there are no states of selfstress surrounding the holes. This is shown by taking the covering tiles of the two holes, for which the red line in the figure indicates how far these tiles reach into the tiling. When using Algorithm 1, we find that this tiling has no states of selfstress surrounding the holes. Consequently, the only states of selfstress in this tiling are the local 3×3 states of selfstress.

In contrast to the example in Figure 4.6, the example in Figure 4.7 is a tiling in which it is possible to find states of selfstress surrounding these holes.

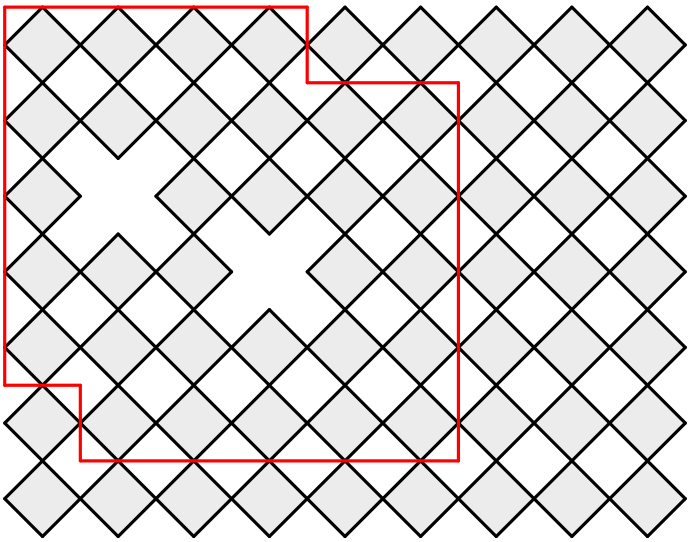

Figure 4.7: The 7×9 tiling with the tiles at $(3, 2)$ and $(4, 4)$ removed. Again, all tiles that are covered by 3×3 states of selfstress over the holes are surrounded by the red boundary. For this tiling, we have $N = 61$, $B = 40$ and $n_{ZM} = 4$, and thus this gives $n_{SSS} = 25$.

Just like the example in Figure 4.6, we try to find the states of selfstress on the tiling that is surrounded by the red coloured boundary using Algorithm 1. This algorithm gives that there exist three states of selfstress surrounding these holes, namely the three states of selfstress depicted in Figure 4.8. All of these states of selfstress are configurations like the one in Figure 3.22, one is exactly the same state of selfstress, the other two are a combination of this state of selfstress on a bigger hole and 3×3 states of selfstress. Apart from these three states of selfstress, the tiling also contains 22 3×3 states of selfstress.

Thus, in general, for any given tiling, we first look whether we can split up this tiling into multiple smaller tilings, as described in 4.2, because of a boundary that is at least two tiles broad. After this, we can either see whether the different subtilings contain a single hole, or multiple holes. In both cases, if we do not see an 'easy' solution to the problem of finding the states of selfstress in the subtiling, these states can be obtained by applying Algorithm 1.

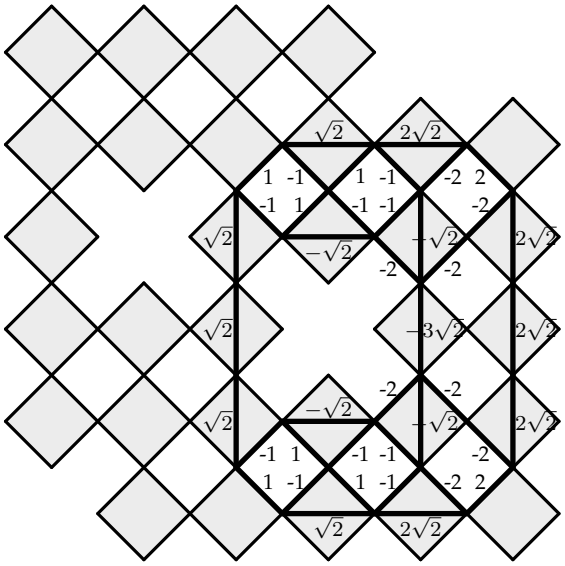

(a) The first state of selfstress in the subtiling of Figure 4.7 surrounded by the red line, is equivalent to the state of selfstress in the tiling in Figure 3.22.

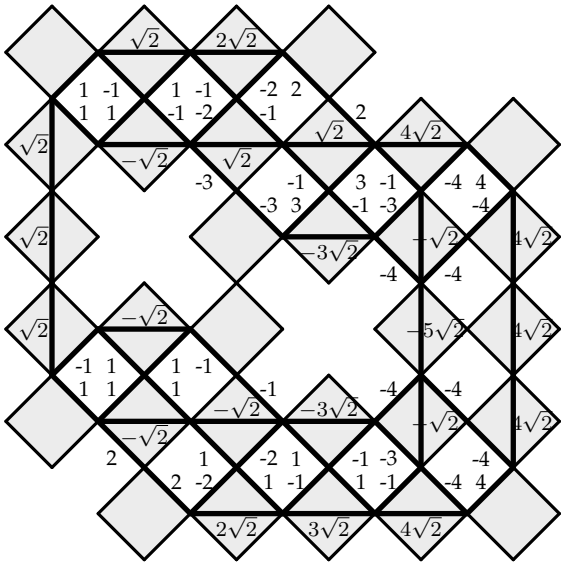

(b) The second state of selfstress is a variant of the state of selfstress in the tiling in Figure 3.22, but has a larger hole.

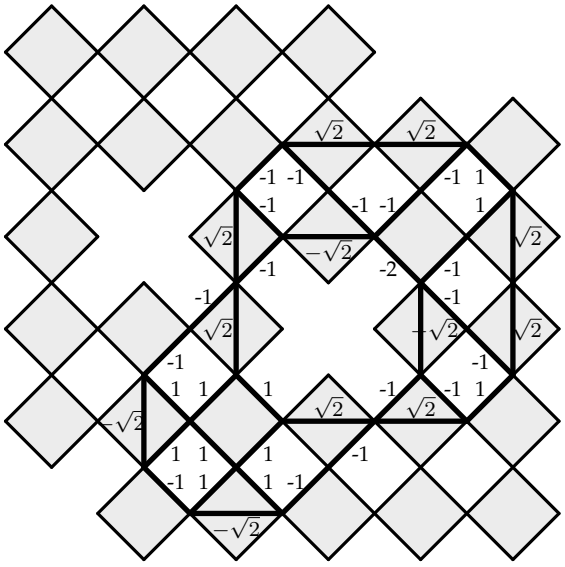

(c) The third state of selfstress is a state of stelfstress that has not been considered before, but is surrounding one of the holes.

Figure 4.8: The states of selfstress in the subtiling of the 7×9 tiling, surrounded by the red line. In these tilings all tiles of the 7×9 tiling, except the tiles that are part of the states of selfstress covering the holes at $(3, 2)$ and $(4, 4)$), are removed.

Chapter 5

Breaking corners

5.1 Breaking apart connected corners in the tiling

The reasoning in the previous chapters does not only apply when tiles are removed, but also when bonds between tiles are broken. In this case, the algorithm to solve the problem is similar to Algorithm 1, with the adaptation that the bonds that are considered in the set S, the set of bonds on which there is a zero force, are the bonds that are broken, and the set T is empty, since no tiles are removed. This will be shown for the example in Figure 5.1.

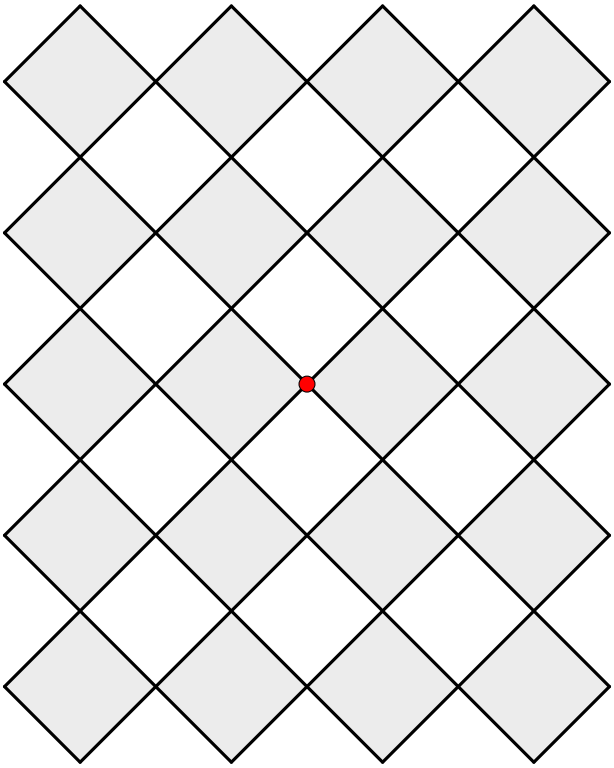

Figure 5.1: A tiling in which the bonds between the two tiles in the center (the bond at the corner denoted in red) is broken.

In this example, the state of selfstress again surrounds the removed bond. This state of selfstress is depicted in Figure 5.2, and the corresponding 3×3 representation is $\vec{c} = \begin{bmatrix} 1 & 1 \\ 1 & 1 \\ 1 & 1 \end{bmatrix}$.

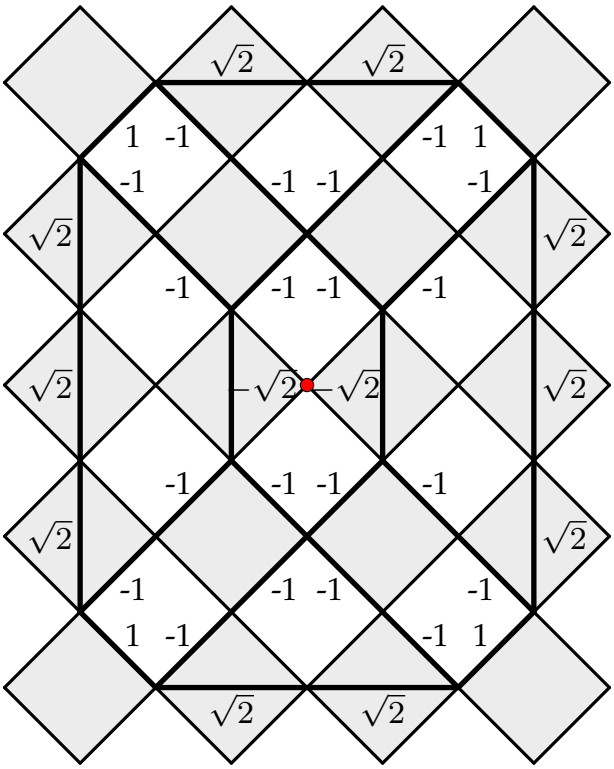

Figure 5.2: The state of selfstress obtained in the tiling of Figure 5.1. This state of selfstress surrounds the broken bond in the tiling.

The approach in Sections 4.2 and 4.3 can be extended to larger tilings containing holes, bonds that are broken and combinations of these two. Thus, this extends the reasoning and the algorithm to any other tiling, resulting in finding all states of selfstress of the system.

Chapter 6

Discussion

In this thesis, we have discussed how to find states of selfstress in tilings and have given several examples of tilings on which we have found states of selfstress. The importance of finding these states of selfstress is to know everything about the intrinsic properties of the materials, thus implying the knowledge of for example the number of states of selfstress or zero modes in the system and where these can be found. We have considered a relatively easy way to determine the states of selfstress in the tiling, and shown that this can be applied to a lot of examples. With this algorithm, the states of selfstress in the tiling can be determined quickly, also giving the number of zero modes in the system.

In general, we have considered a large amount of the states of selfstress around single holes. Of course, there are more examples of tilings that we have not considered, due to a removal of different tiles at the boundary. If tiles at the boundary are removed, the covering states of selfstress containing these tiles can no longer be used to find a state of selfstress. In this case it is possible to get states of selfstress over smaller tilings, like the one shown in Figure 4.8c. For these tilings, there might exist more states of selfstress that are not considered in this thesis, but these are all relatively easy to find.

For bonds that are broken, this thesis also considers just one example. Of course, there are a lot of other examples for this problem that we have not considered in this thesis. On the other hand, it is again easy to find the states of selfstress in these problems, either by making a smart guess, or using the algorithm. Equivalently, this can be done for states of selfstress on tilings with combinations of multiple holes and broken bonds, for which we have given no examples, but for which it is also relatively easy to find states of selfstress.

Apart from these perfect squares that are located next to each other, we could also consider tiles that are hinged with respect to each other, and consider what the states of selfstress look like in these tilings, and if they are comparable to the states of selfstress in the original tiling. In this case it is relatively easy to find the states of selfstress in the tiling. It is also possible to distort the shape of the tiles a little bit, in such a way that the tiles are still connected at the corners. After this distortion, it is possible to consider the states of selfstress on the tilings, and look whether these are related to the original states of selfstress. Further research needs to be done to examine whether this is the case.

Appendix A

Definitions

All of the following definitions are already mentioned in de above chapters, but are mentioned here as a quick back-up, since some of the definitions are used often, but explained only once.

A **bond** or **connection** is the attachment point of two connected tiles in the tiling. Page 9

The 3×3 **covering states of selfstress** are the the 3×3 states of selfstress containing a part of the holes and contributing to the larger state of selfstress. Page 26

States of selfstress that are located on 3×3 tilings, are called 3×3 *subtilings* or *(local)* 3×3 *states of selfstress*. Page 26

A **basis state of selfstress** is a state of selfstress that can not be written as a linear combination of two states of selfstress on smaller tilings, i.e. tilings containing less squares. Page 24

A restriction on the properties of different objects in a system is called a **constraint**. Page 8

The **degrees of freedom (or DOF)** are the parameters in a system that can change independently of each other. The number of independent degrees of freedom will be denoted by n_{DOF}. Page 7

The **global zero modes** are defined as the two translational and one rotational zero mode intrinsic to the system. Page 8

The **local zero modes** are the additional zero modes, these are internal to the system. These are additional to the global zero modes. Page 8

A system will be called a **mechanism**, in the case that there is only one zero mode in the system. Page 8.

The **number of zero modes, free modes, relative mobility of mobility**, is defined as the number of independent parameters that can change without violating the constraints. The number of independent zero modes is denoted by n_{ZM}. Page 8

The **polygon boundary** is the smallest binding polygon with horizontal and vertical edges, for which both endpoints of the edges are in the centres of (expected) holes. Page 24

A **state of selfstress** in a system is a combination of forces over the elements in the system, that add up to a net force of zero. Page 8

Acknowledgements

I mostly would like to thank my supervisors for their time an the effort they have put into making my thesis as wonderful as it is now. Martin, thanks for giving me the subject and pointing me in the right directions when I did not know which problem to address. Anne, thank you for giving me a general guideline and helping me through the already-known by others, sometimes difficult, theoretical parts of this thesis. Floske, thank you for all the re-reading and giving advice to make it better. Even in incredibly busy periods you still made lots of time to read my thesis and spend hours of talking about both my thesis and a lot of other, sometimes a little less relevant, subjects. I really enjoyed these hours.

I would also like to thank my fellow board members of De Leidsche Flesch. Even though I did not see time to spend on my thesis at some points, they have told me more than once to take days off to work on it, which I then of course did not do. I am happy that I had to spend my full last year on the university with you, to have fun and a mutual chronic lack of sleep. Dennis, Joost, Rémi, Wout and Erik, thank you so much!

Finally, I would like to thank my parents, for always supporting me my entire life. Although the last year was really difficult sometimes, I really liked coming back to you and have a distraction from the things that stayed on my mind all the time.

Bibliography

[1] C.R. Calladine. Buckminster fuller's 'tensegrity' structures and clerk maxwell's rules for the construction of stiff frames. *International Journal of Solids and Structures*, 14(2):161 – 172, 1978.

[2] Johan Christensen, Muamer Kadic, Oliver Kraft, and Martin Wegener. Vibrant times for mechanical metamaterials. *MRS Communications*, 5:453–462, 2015.

[3] K.H. Hunt. *Kinematic geometry of mechanisms*, volume 7. Oxford University Press, USA, 1978.

[4] R. S. Lakes. Negative poisson's ratio materials. `http://silver.neep.wisc.edu/~lakes/Poisson.html`. Accessed: July 23, 2018.

[5] R. S. Lakes. Foam structures with a negative poisson's ratio. *Science*, 235(4792):1038–1040, 1987.

[6] L.A. Lubbers. *Mechanical Metamaterials: Nonlinear Beams and Excess Zero Modes*. PhD thesis, Leiden University, 2018.

[7] A.S. Meeussen. Topological principles for the design of mechanical metamaterials, 2016. Master's thesis at Leiden University.

[8] A.S. Meeussen, 2018. (Notes on Shearing Deformations.).

[9] S. Pellegrino and C.R. Calladine. Matrix analysis of statically and kinematically indeterminate frameworks. *International Journal of Solids and Structures*, 22(4):409–428, 1986.

[10] M. van Hecke. Counting symmetric & generic quads, 2017. (Notes of counting states of selfstress).